Prior and Posterior Networks: A Survey on Evidential Deep Learning Methods For Uncertainty Estimation

Anonymous authors
Paper under double-blind review

Abstract

Popular approaches for quantifying predictive uncertainty in deep neural networks often involve distributions over weights or multiple models, for instance via Markov Chain sampling, ensembling, or Monte Carlo dropout. These techniques usually incur overhead by having to train multiple model instances or do not produce very diverse predictions. This comprehensive and extensive survey aims to familiarize the reader with an alternative class of models based on the concept of *Evidential Deep Learning*: For unfamiliar data, they admit "what they don't know" and fall back onto a prior belief. Furthermore, they allow uncertainty estimation in a single model and forward pass by parameterizing *distributions over distributions*. This survey recapitulates existing works, focusing on the implementation in a classification setting, before surveying the application of the same paradigm to regression. We also reflect on the strengths and weaknesses compared to other existing methods and provide the most fundamental derivations using a unified notation to aid future research.

1 Introduction

Many existing methods for uncertainty estimation leverage the concept of Bayesian model averaging: These include ensembling (Lakshminarayanan et al., 2017; Wilson & Izmailov, 2020), Markov chain Monte Carlo sampling (de Freitas, 2003; Andrieu et al., 2000) as well as variational inference approaches (Mackay, 1992; MacKay, 1995; Hinton & Van Camp, 1993; Neal, 2012), including approaches such as Monte Carlo (MC) dropout (Gal & Ghahramani, 2016) and Bayes-by-backprop (Blundell et al., 2015). Bayesian model averaging involves the approximation of an otherwise infeasible integral using MC samples. This causes the following problems: Firstly, the quality of the MC approximation depends on the veracity and diversity of samples from the weight posterior. Secondly, the approach often involves increasing the number of parameters in a model or training more model instances altogether. Recently, a new class of models has been proposed to side-step this conundrum by using a different factorization of the posterior predictive distribution. This allows computing uncertainty in a single forward pass and with a single set of weights. These models are grounded in a concept coined *Evidential Deep Learning*: For out-of-distribution (OOD) inputs, they fall back onto a prior. This is often described as *knowing what they don't know*.

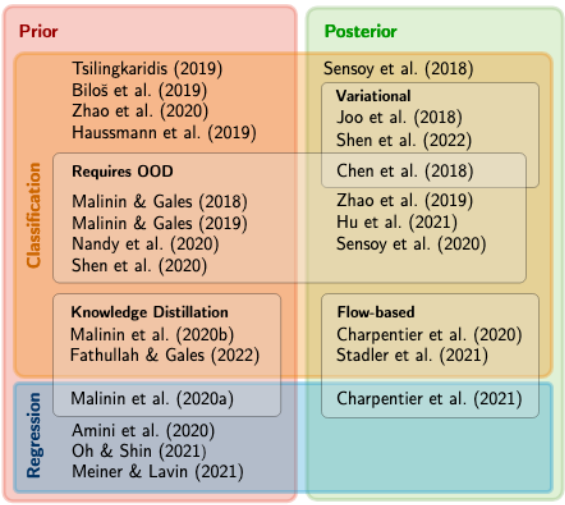

Figure 1: Taxonomy of surveyed approaches, divided into tractable parameterizations of the prior or posterior on one axis (see Tables 1 and 2 for an overview) and into approaches for classification and regression on the other. Regression methods are outlined in Table 3.

In this paper, we summarize the existing literature and provide an overview of Evidential Deep Learning approaches. We give an overview over all discussed work in Figure 1, where we distinguish surveyed works for classification between models parameterizing a Dirichlet prior (Section 3.4.1) or posterior (Section 3.4.2). We further discuss similar methods for regression problems (Section 4). As we will see, obtaining well-behaving uncertainty estimates can be challenging in the Evidential Deep Learning framework; proposed solutions that are also reflected in Figure 1 are the usage of OOD examples during training (Malinin & Gales, 2018; 2019; Nandy et al., 2020; Shen et al., 2020; Chen et al., 2018; Zhao et al., 2019; Hu et al., 2021; Sensoy et al., 2020), knowledge distillation (Malinin et al., 2020b;a) or the incorporation of density estimation (Charpentier et al., 2020; 2022; Stadler et al., 2021), which we discuss in more detail in Section 6. This survey aims to both serve as an accessible introduction to this model family to the unfamiliar reader as well as an informative overview, in order to promote a wider application outside the uncertainty quantification literature. We also provide a collection of the most important derivations for the Dirichlet distribution for Machine Learning, which plays a central role in many of the discussed approaches.

2 Background

We first introduce the central concepts for this survey, including Bayesian inference in Section 2.1, Bayesian model averaging in Section 2.2 and Evidential Deep Learning in Section 2.3.

2.1 Bayesian Inference

The foundation of the following sections is Bayesian inference: Given some prior belief $p(\boldsymbol{\theta})$ about parameters of interest $\boldsymbol{\theta}$, we use available observations $\mathbb{D} = \{(x_i, y_i)\}_{i=1}^N$ and their likelihood $p(\mathbb{D}|\,\boldsymbol{\theta})$ to obtain an updated belief in form of the posterior $p(\boldsymbol{\theta}\,|\mathbb{D}) \propto p(\mathbb{D}|\,\boldsymbol{\theta})p(\boldsymbol{\theta})$. This update rule is derived from Bayes' rule, namely

$$p(\boldsymbol{\theta}\,|\mathbb{D}) = \frac{p(\mathbb{D}|\,\boldsymbol{\theta})p(\boldsymbol{\theta})}{p(\mathbb{D})} = \frac{p(\mathbb{D}|\,\boldsymbol{\theta})p(\boldsymbol{\theta})}{\int p(\mathbb{D}|\,\boldsymbol{\theta})p(\boldsymbol{\theta})d\,\boldsymbol{\theta}}, \tag{1}$$

where we often try to avoid computing the term in the denominator since marginalization over a large (continuous) parameter space of $\boldsymbol{\theta}$ is usually intractable. In order to perform a prediction y for a new data point $\mathbf{x}$, we can now utilize the *posterior predictive distribution* defined as

$$P(y|\,\mathbf{x}, \mathbb{D}) = \int P(y|\,\mathbf{x}, \boldsymbol{\theta})p(\boldsymbol{\theta}|\mathbb{D})d\boldsymbol{\theta}. \tag{2}$$

Since we integrate over the entire parameter space of $\boldsymbol{\theta}$, weighting each prediction by the posterior probability of its parameters to obtain the final result, this process is referred to as *Bayesian model averaging* (BMA). Here, predictions $P(y|\,\mathbf{x}, \boldsymbol{\theta})$ stemming from parameters that are plausible given the observed data will receive a higher weight $p(\boldsymbol{\theta}|\mathbb{D})$ in the final prediction $P(y|\,\mathbf{x}, \mathbb{D})$. As we will see in the following section, this factorization of the predictive predictive distribution also has beneficial properties for analyzing the uncertainty of a model.

2.2 Predictive Uncertainty in Neural Networks

In probabilistic modelling, uncertainty is commonly divided into aleatoric and epistemic uncertainty (Der Kiureghian & Ditlevsen, 2009; Kendall & Gal, 2017; Hüllermeier & Waegeman, 2021). Aleatoric uncertainty refers to the uncertainty that is induced by the data-generating process, for instance noise or inherent overlap between observed instances of classes. Epistemic uncertainty is the type of uncertainty about the optimal model parameters (or even hypothesis class). It is reducible with an increasing amount of data, as fewer and fewer possible models become a plausible fit. These two notions resurface when formulating the posterior predictive distribution for a new data point $\mathbf{x}$:[1]

[1]Note that the predictive distribution in Equation (2) generalizes the common case for a single network prediction where $P(y|\,\mathbf{x}, \boldsymbol{\theta}) \approx P(y|\,\mathbf{x}, \hat{\boldsymbol{\theta}})$. Mathematically, this is expressed by replacing the posterior $p(\boldsymbol{\theta}|\mathbb{D})$ by a Dirac delta distribution as in Equation (5), where all probability density rests on a single parameter configuration.

$$P(y|\,\mathbf{x},\mathbb{D}) = \int \underbrace{P(y|\,\mathbf{x},\boldsymbol{\theta})}_{\text{Aleatoric}}\ \underbrace{p(\boldsymbol{\theta}|\mathbb{D})}_{\text{Epistemic}}\ d\boldsymbol{\theta}. \tag{3}$$

Here, the first factor captures the aleatoric uncertainty about the correct prediction, while the second one expresses uncertainty about the correct model parameters—the more data we observe, the more density of $p(\boldsymbol{\theta}|\mathbb{D})$ should lie on reasonable parameter values for $\boldsymbol{\theta}$. For high-dimensional real-valued parameters $\boldsymbol{\theta}$ like in neural networks, this integral becomes intractable, and is usually approximated using Monte Carlo samples:

$$P(y|\,\mathbf{x},\mathbb{D}) \approx \sum_{k=1}^{K} P(y|\,\mathbf{x},\boldsymbol{\theta}^{(k)}) \tag{4}$$

based on K different sets of parameters $\boldsymbol{\theta}^{(k)}$. Since this requires obtaining multiple versions of model parameters through some additional procedure, this however comes with the aforementioned problems of computational overhead and approximation errors, motivating the approaches discussed in this survey.

2.3 Evidential Deep Learning

Since the traditional approach to predictive uncertainty estimation requires multiple parameter sets and can only approximate the predictive posterior, we can factorize Equation (2) further to obtain a tractable form:

$$p(y|\,\mathbf{x},\mathbb{D}) = \iint \underbrace{P(y|\boldsymbol{\mu})}_{\text{Aleatoric}}\ \underbrace{p(\boldsymbol{\mu}|\,\mathbf{x},\boldsymbol{\theta})}_{\text{Distributional}}\ \underbrace{p(\boldsymbol{\theta}|\mathbb{D})}_{\text{Epistemic}}\ d\boldsymbol{\mu}d\boldsymbol{\theta} \approx \int P(y|\boldsymbol{\mu})\ \underbrace{p(\boldsymbol{\mu}|\,\mathbf{x},\hat{\boldsymbol{\theta}})}_{p(\boldsymbol{\theta}|\mathbb{D})\approx\delta(\boldsymbol{\theta}-\hat{\boldsymbol{\theta}})}\ d\boldsymbol{\mu}. \tag{5}$$

This factorization contains another type of uncertainty, which the authors call the *distributional* uncertainty, uncertainty caused by the mismatch of training and test data distributions. In the last step, Malinin & Gales (2018) replace $p(\boldsymbol{\theta}|\mathbb{D})$ by a point estimate $\hat{\boldsymbol{\theta}}$ using the Dirac delta function, i.e. a single trained neural network, to get rid of the intractable integral. Although another integral remains, retrieving the uncertainty from this predictive distribution actually has a closed-form analytical solution for the Dirichlet (see Section 3.3). The advantage of this approach is further that it allows us to distinguish uncertainty about a data point because it is ambiguous from points coming from an entirely different data distribution. As an example, consider a binary classification problem, in which the data manifold consists of two overlapping clusters. As we are classifying a new data point, we obtain a distribution $P(y|\,\mathbf{x},\boldsymbol{\theta})$ which is uniform over the two classes. What does this mean? The model might either be confident that the point lies in the region of overlap and is inherently ambiguous, or that the model is uncertain about the correct class. Without further context, we cannot distinguish between these two cases (Bengs et al., 2022; Hüllermeier, 2022). Compare that to instead predicting $p(\boldsymbol{\mu}|\,\mathbf{x},\boldsymbol{\theta})$: If the data point is ambiguous, the resulting distribution will be centered on 0.5, if the model is generally uncertain, the distribution will be uniform, allowing this distinction. We will illustrate this principle further in the upcoming Sections 2.4 and 3.3.

In the neural network context in Equation (5), it should be noted that restricting oneself to a point estimate of the parameters prevent the estimation of epistemic uncertainty like in earlier works through the weight posterior $p(\boldsymbol{\theta}|\mathbb{D})$, as discussed in the next section. However, there are works like Haussmann et al. (2019); Zhao et al. (2020) that combine both approaches.

The term *Evidential Deep Learning* (EDL) originates from the work of Sensoy et al. (2018) and is based on the *Theory of Evidence* (Dempster, 1968; Audun, 2018): Within the theory, belief mass is assigned to set of possible states, e.g. class labels, and can also express a lack of evidence, i.e. an "I don't know". We can for instance generalize the predicted output of a neural classifier using the Dirichlet distribution, allowing us to express a lack of evidence through a uniform Dirichlet. This is different from a uniform categorical distribution, which does not distinguish an equal probability for all classes from the lack of evidence. For the purpose of this survey, we define Evidential Deep Learning as a family of approaches in which a neural

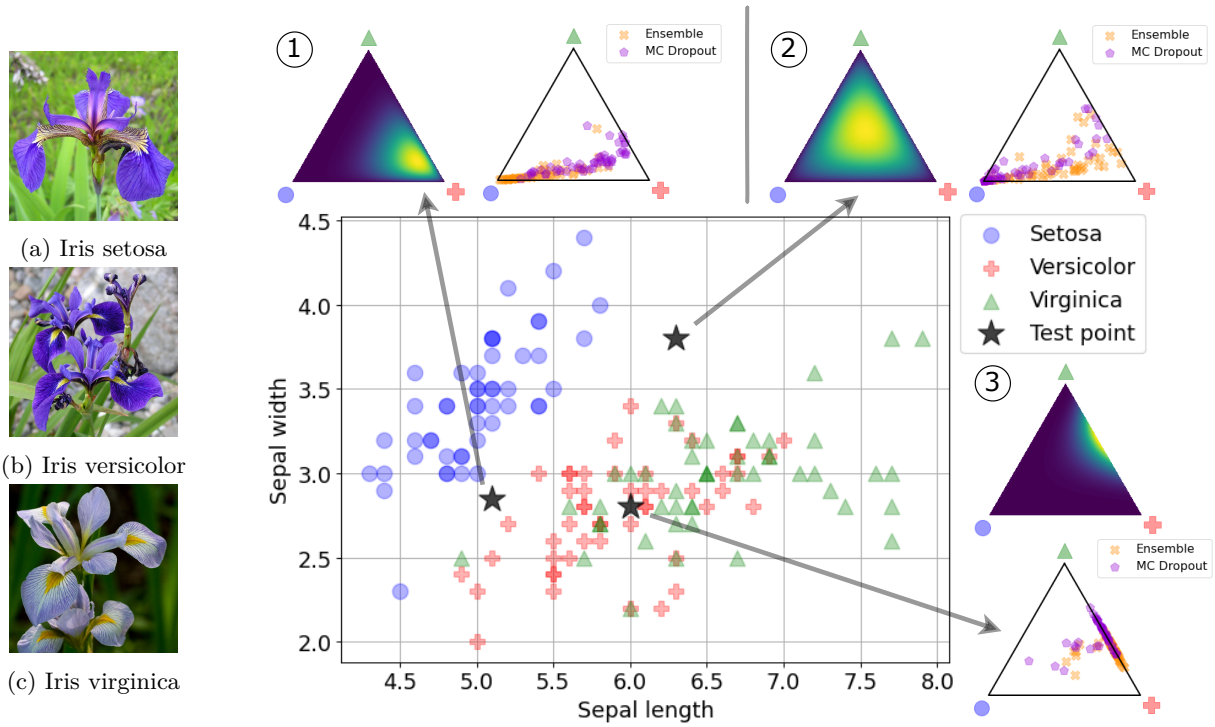

Figure 2: Illustration of different approaches to uncertainty quantifying on the Iris dataset, with examples for the classes given on the left (Figures 2a to 2c). On the right, the data is plotted alongside some predictions of a prior network (lighter colors indicate higher density) and an ensemble and MC Dropout model on the probability simplex, with 50 predictions each. Iris images were taken from Wikimedia Commons, 2022a;b;c.

network can fall back onto a uniform prior for unknown inputs. While neural networks usually parameterize likelihood functions, approaches in this survey parameterize prior or posterior distributions instead. The advantages of this methodology are now demonstrated using the example in the following section.

2.4 An Illustrating Example: The Iris Dataset

To illustrate the advantages of EDL, we choose a classification problem based on the Iris dataset (Fisher, 1936). It contains measurements of three different species of iris flowers (shown in Figures 2a to 2c). We use the dataset as made available through `scikit-learn` (Pedregosa et al., 2011) and plot the relationship between the width and lengths measurements of the flowers' petals in Figure 2.

We train an deep neural network ensemble (Lakshminarayanan et al., 2017) with 50 model instances, a model with MC Dropout (Gal & Ghahramani, 2016) with 50 predictions and a prior network (Sensoy et al., 2018), an example of EDL, on all available data points, and plot their predictions on three test points on the 3-probability simplex in Figure 2.[2] On these simplices, each point signifies a categorical distribution, with the proximity to one of the corners indicating a higher probability for the corresponding class. EDL methods for classification do not predict a single output distribution, but an entire *density over output distributions*.

Test point ③ lies in a region of overlap between instances of Iris versicolor and Iris virginica, thus inducing high aleatoric uncertainty. In this case, we can see that the prior network places all of its density on between these two classes, similar to most of the predictions of the ensemble and MC Dropout (bottom right). However, some of the latter predictions still land in the center of the simplex. The point ① is located in an area without training examples between instances of Iris versicolor and setosa, as well as close to a Single virginica outlier. As shown in the top left, ensemble and MC Dropout predictions agree that the point

[2]For information about training and model details, see Appendix A.1.

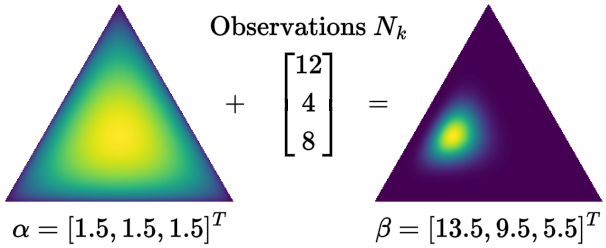

Figure 3: A prior Dirichlet distribution is updated with a vector of class observations. The posterior Dirichlet then shifts density towards the classes k with more observed instances.

belongs to either the setosa or versicolor class, with a slight preference for the former. The prior network concentrates its prediction on versicolor, but admits some uncertainty towards the two other choices. The last test point ② is placed in an area of the feature space devoid of any data, roughly equidistant from the three clusters of flowers. Similar to the previous example, the ensemble and MC dropout predictions on the top right show a preference for Iris setosa and versicolor, albeit with higher uncertainy. The prior network however shows an almost uniform density, admitting distributional uncertainty about this particular input.

This simple example provides some insights into the potential advantages of EDL: First of all, the prior network was able to provide reasonable uncertainty estimates in comparison with BMA methods. Secondly, the prior network is able to admit its lack of knowledge for the OOD data point by predicting an almost uniform prior, something that the other models are not able to. As laid out in Section 3.3, EDL actually allows the user to disentangle model uncertainty due to a simple lack of data and due to the input being out-of-distribution. Lastly, training the prior network only required a single model, which is a noticeable speed-up compared to MC Dropout and especially the training of ensembles.

3 Dirichlet Networks

In order to introduce Dirichlet networks, we first give a brief introduction to the Dirichlet distribution and its role as a conjugate prior in Bayesian inference in Section 3.1. We then show in Section 3.2 how neural networks can parameterize Dirichlet distributions, while Section 3.3 reveals how such a parameterization can be exploited for efficient uncertainty estimation. The remaining sections enumerate different examples from the literature parameterizing either a prior (Section 3.4.1) or posterior Dirichlet distribution (Section 3.4.2).

3.1 The Dirichlet distribution

Modelling for instance a binary classification problem is commonly done using the Bernoulli likelihood. The Bernoulli likelihood has a single parameter μ, indicating the probability of success (or of the positive class), and is given by

$$\text{Bernoulli}(y|\mu) = \mu^y (1-\mu)^{(1-y)}. \tag{6}$$

Within Bayesian inference as introduced in Section 2, the Beta distribution is a commonly used prior for a Bernoulli likelihood. It defines a probability distribution over the parameter μ, itself possessing two shape parameters α_1 and α_2:

$$\text{Beta}(\mu; \alpha_1, \alpha_2) = \frac{1}{B(\alpha_1, \alpha_2)} \mu^{\alpha_1 - 1} (1-\mu)^{\alpha_2 - 1}; \quad B(\alpha_1, \alpha_2) = \frac{\Gamma(\alpha_1)\Gamma(\alpha_2)}{\Gamma(\alpha_1 + \alpha_2)}; \tag{7}$$

where $\Gamma(\cdot)$ stands for the gamma function, a generalization of the factorial to the real numbers, and $B(\cdot)$ is called the Beta function (not to be confused with the distribution). When extending the classification problem to from two to an arbitrary number of classes, we use a Categorical likelihood:

$$\text{Categorical}(y|\boldsymbol{\mu}) = \prod_{k=1}^{K} \mu_k^{\mathbf{1}_{y=k}}, \tag{8}$$

in which K denotes the number of categories or classes, and the class probabilities are expressed using a vector $\boldsymbol{\mu} \in [0,1]^K$ with $\sum_k \mu_k = 1$, and $\mathbf{1}_{(\cdot)}$ is the indicator function. This distribution appears for instance in classification problems when using neural networks, since most neural networks for classification use a softmax function after their last layer to produce a categorical distribution of classes s.t. $\mu_k \equiv P(y = k|x)$. In this setting, the Dirichlet distribution arises as a suitable prior and multivariate generalization of the Beta distribution (and is thus also called the *multivariate Beta distribution*):

$$\text{Dir}(\boldsymbol{\mu}; \boldsymbol{\alpha}) = \frac{1}{B(\boldsymbol{\alpha})} \prod_{k=1}^{K} \mu_k^{\alpha_k - 1}; \quad B(\boldsymbol{\alpha}) = \frac{\prod_{k=1}^{K} \Gamma(\alpha_k)}{\Gamma(\alpha_0)}; \quad \alpha_0 = \sum_{k=1}^{K} \alpha_k; \quad \alpha_k \in \mathbb{R}^+; \tag{9}$$

where the Beta function $B(\cdot)$ is now defined for K shape parameters compared to Equation (7). For notational convenience, we also define $\mathbb{K} = \{1, \ldots, K\}$ as the set of all classes. The distribution is characterized by its *concentration parameters* $\boldsymbol{\alpha}$, the sum of which, often denoted as α_0, is called the *precision*.[3] The Dirichlet is a *conjugate prior* for such a categorical likelihood, meaning that according to Bayes' rule in Equation (1), they produce a Dirichlet posterior with parameters $\boldsymbol{\beta}$, given a data set $\mathbb{D} = \{(x_i, y_i)\}_{i=1}^N$ of N observations with corresponding labels:

$$\begin{aligned} p(\boldsymbol{\mu}|\mathbb{D}, \boldsymbol{\alpha}) \propto p\big(\{y_i\}_{i=1}^N | \boldsymbol{\mu}, \{x_i\}_{i=1}^N\big) p(\boldsymbol{\mu}|\boldsymbol{\alpha}) &= \prod_{i=1}^{N} \prod_{k=1}^{K} \mu_k^{\mathbf{1}_{y_i=k}} \frac{1}{B(\boldsymbol{\alpha})} \prod_{k=1}^{K} \mu_k^{\alpha_k - 1} \\ &= \prod_{k=1}^{K} \mu_k^{\left(\sum_{i=1}^{N} \mathbf{1}_{y_i=k}\right)} \frac{1}{B(\boldsymbol{\alpha})} \prod_{k=1}^{K} \mu_k^{\alpha_k - 1} = \frac{1}{B(\boldsymbol{\alpha})} \prod_{k=1}^{K} \mu_k^{N_k + \alpha_k - 1} \propto \text{Dir}(\boldsymbol{\mu}; \boldsymbol{\beta}), \end{aligned} \tag{10}$$

where $\boldsymbol{\beta}$ is a vector with $\beta_k = \alpha_k + N_k$, with N_k denoting the number of observations for class k. Intuitively, this implies that the prior belief encoded by the initial Dirichlet is updated using the actual data, sharpening the distribution for classes for which many instances have been observed. Similar to the Beta distribution in Equation (7), the Dirichlet is a *distribution over categorical distributions* on the $K - 1$ probability simplex; we show an example with its concentration parameters and the Bayesian update in Figure 3.

3.2 Parameterization

For a classification problem with K classes, a neural classifier is usually realized as a function $f_{\boldsymbol{\theta}} : \mathbb{R}^D \to \mathbb{R}^K$, mapping an input $\mathbf{x} \in \mathbb{R}^D$ to *logits* for each class. Followed by a softmax function, this then defines a categorical distribution over classes with a vector $\boldsymbol{\mu}$ with $\mu_k \equiv p(y = k|\, \mathbf{x}, \boldsymbol{\theta})$. The same underlying architecture can be used without any major modification to instead parameterize a *Dirichlet* distribution, predicting a distribution *over categorical distributions* $p(\boldsymbol{\mu}|\, \mathbf{x}, \hat{\boldsymbol{\theta}})$ as in Equation (9).[4] In order to classify a data point $\mathbf{x}$, a categorical distribution is created from the predicted concentration parameters of the Dirichlet as follows (this corresponds to the mean of the Dirichlet, see Appendix C.1):

$$\boldsymbol{\alpha} = f_{\boldsymbol{\theta}}(\mathbf{x}); \quad \mu_k = \frac{\alpha_k}{\alpha_0}; \quad \hat{y} = \arg\max_{k \in \mathbb{K}} \ \mu_1, \ldots, \mu_K. \tag{11}$$

Parameterizing a Dirichlet posterior distribution follows a similar logic, as we will discuss in Section 3.4.2.

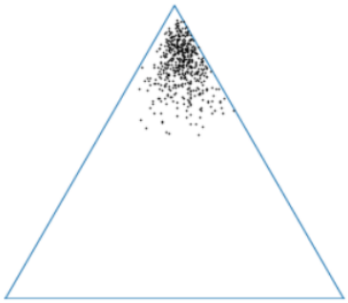

(a) Categorical distributions predicted by a neural ensemble on the probability simplex.

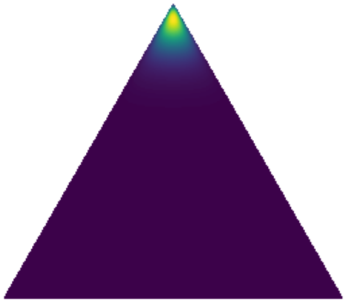

(b) Probability simplex for a confident prediction, for with the density concentrated in a single corner.

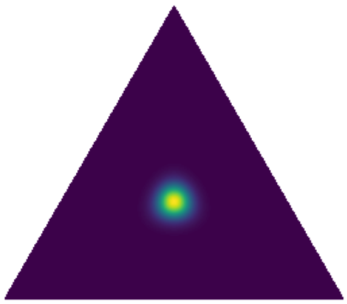

(c) Dirichlet distribution for a case of data uncertainty, with the density concentrated in the center.

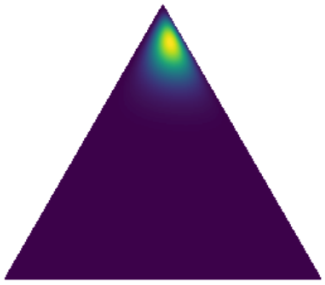

(d) Dirichlet distribution for a case of model uncertainty, with the density spread out more.

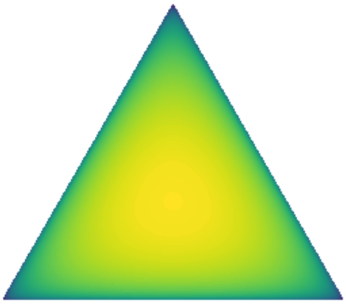

(e) Dirichlet for a case of distributional uncertainty, with the density spread across the whole simplex.

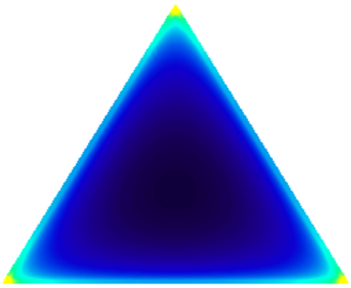

(f) Alternative approach to distributional uncertainty called representation gap, with density concentrated along the edges.

Figure 4: Examples of the probability simplex for a $K = 3$ classification problem, where every corner corresponds to a class and every point to a categorical distribution. Brighter colors correspond to higher density. (a) Predicted categorical distributions by an ensemble of discriminators. (b) – (e) (Desired) Behavior of Dirichlet in different scenarios by Malinin & Gales (2018): (b) For a confident prediction, the density is concentrated in the corner of the simplex corresponding to the assumed class. (c) In the case of aleatoric uncertainty, the density is concentrated in the center, and thus uniform categorical distributions are most likely. (d) In the case of model uncertainty, the density may still be concentrated in a corner, but more spread out, expressing the uncertainty about the right prediction. (e) In the case of an OOD input, a uniform Dirichlet expresses that any categorical distribution is equally likely, since there is no evidence for any known class. (f) Representation gap by Nandy et al. (2020), proposed as an alternative behavior for OOD data. Here, the density is instead concentrated solely on the edges of the simplex.

3.3 Uncertainty Estimation with Dirichlet Networks

Let us now turn our attention to how to estimate the aleatoric, epistemic and distributional uncertainty as laid out in Section 2.2 within the Dirichlet framework. In Figure 4, we show different shapes of a Dirichlet distribution parameterized by a neural network, corresponding to different cases of uncertainty, where each point on the simplex represents a categorical distribution, with proximity to a corner indicating a high probability for the corresponding class. Figure 4a displays the predictions of an ensemble of classifiers as a point cloud on the simplex. Using a Dirichlet, this finite set of distributions can be extended to a continuous density over the whole simplex. As we will see in the following sections, parameterizing a

[3]The precision is analogous to the precision of a Gaussian, where a larger α_0 signifies a sharper distribution.

[4]The only thing to note here is that the every α_k has to be strictly positive, which can for instance be enforced by using an additional softplus, exponential or ReLU function (Sensoy et al., 2018; Malinin & Gales, 2018; Sensoy et al., 2020).

Dirichlet distribution with a neural network enables us to distinguish different scenarios using the shape of its density, as shown in Figures 4b to 4f, which we will discuss in more detail along the way.

However, since we do not want to inspect Dirichlets visually, we instead use closed form expression to quantify uncertainty, which we will discuss now. Although stated for the prior parameters $\boldsymbol{\alpha}$, the following methods can also be applied to the posterior parameters $\boldsymbol{\beta}$ without loss of generality.

Data (aleatoric) uncertainty To obtain a measure of data uncertainty, we can evaluate the expected entropy of the data distribution $p(y|\boldsymbol{\mu})$ (similar to previous works like e.g. Gal & Ghahramani, 2016). As the entropy captures the "peakiness" of the output distribution, a lower entropy indicates that the model is concentrating most probability mass on a single class, while high entropy characterizes a more uniform distribution—the model is undecided about the right prediction. For Dirichlet networks, this quantity has a closed-form solution (for the full derivation, refer to Appendix D.1):

$$\mathbb{E}_{p(\boldsymbol{\mu}|\,\mathbf{x},\hat{\boldsymbol{\theta}})}\Big[H\Big[P(y|\boldsymbol{\mu})\Big]\Big] = -\sum_{k=1}^{K}\frac{\alpha_k}{\alpha_0}\Big(\psi(\alpha_k+1)-\psi(\alpha_0+1)\Big) \tag{12}$$

where ψ denotes the digamma function, defined as $\psi(x) = \frac{d}{dx}\log\Gamma(x)$, and H the Shannon entropy.

Model (epistemic) uncertainty As we saw in Section 2.2, most approaches in the Dirichlet framework avoid the intractable integral over network parameters $\boldsymbol{\theta}$ by using a point estimate $\hat{\boldsymbol{\theta}}$.[5] This means that computing the model uncertainty via the weight posterior $p(\boldsymbol{\theta}|\mathbb{D})$ like in Blundell et al. (2015); Gal & Ghahramani (2016); Smith & Gal (2018) is not possible. Nevertheless, a key property of Dirichlet networks is that epistemic uncertainty is expressed in the spread of the Dirichlet distribution (for instance in Figure 4 (d) and (e)). Therefore, the epistemic uncertainty can be quantified considering the concentration parameters $\boldsymbol{\alpha}$ that shape this distribution: Charpentier et al. (2020) simply consider the maximum α_k as a score akin to the maximum probability score by Hendrycks & Gimpel (2017), while Sensoy et al. (2018) compute it by $K/\sum_{k=1}^{K}(\alpha_k+1)$ or simply α_0 (Charpentier et al., 2020). In both cases, the underlying intuition is that larger α_k produce a sharper density, and thus indicate increased confidence in a prediction.

Distributional uncertainty Another appealing property of this model family is being able to distinguish uncertainty due to model underspecification (Figure 4d) from uncertainty due to alien inputs (Figure 4e). In the Dirichlet framework, the distributional uncertainty can be quantified by computing the difference between the total amount of uncertainty and the data uncertainty, which can be expressed through the mutual information between the label y and its categorical distribution $\boldsymbol{\mu}$:

$$I\Big[y,\boldsymbol{\mu}\Big|\,\mathbf{x},\mathbb{D}\Big] = \underbrace{H\Big[\mathbb{E}_{p(\boldsymbol{\mu}|\,\mathbf{x},\mathbb{D})}\Big[P(y|\boldsymbol{\mu})\Big]\Big]}_{\text{Total Uncertainty}} - \underbrace{\mathbb{E}_{p(\boldsymbol{\mu}|\,\mathbf{x},\mathbb{D})}\Big[H\Big[P(y|\boldsymbol{\mu})\Big]\Big]}_{\text{Data Uncertainty}} \tag{13}$$

This quantity expresses how much information we would receive about $\boldsymbol{\mu}$ if we were given the label y, conditioned on the new input $\mathbf{x}$ and the training data $\mathbb{D}$. In regions in which the model is well-defined, receiving y should not provide much new information about $\boldsymbol{\mu}$—and thus the mutual information would be low. Yet, such knowledge should be very informative in regions in which few data have been observed, and there the mutual information would indicate higher model uncertainty. Given that $\mathbb{E}[\mu_k] = \frac{\alpha_k}{\alpha_0}$ (Appendix C.1) and assuming the point estimate $p(\boldsymbol{\mu}|\,\mathbf{x},\mathbb{D}) \approx p(\boldsymbol{\mu}|\,\mathbf{x},\hat{\boldsymbol{\theta}})$ to be sufficient (Malinin & Gales, 2018), we obtain an expression very similar to Equation (12):

$$I\Big[y,\boldsymbol{\mu}\Big|\,\mathbf{x},\mathbb{D}\Big] = -\sum_{k=1}^{K}\frac{\alpha_k}{\alpha_0}\Big(\log\frac{\alpha_k}{\alpha_0}-\psi(\alpha_k+1)+\psi(\alpha_0+1)\Big) \tag{14}$$

[5] With exceptions such as Haussmann et al. (2019); Zhao et al. (2020). When the distribution over parameters in Equation (5) is retained, alternate expressions of the aleatoric and epistemic uncertainty are derived by Woo (2022).

Note on epistemic uncertainty estimation The introduction of distributional uncertainty, a notion that is non-existent in the Bayesian Model Averaging framework, warrants a note on the estimation of epistemic uncertainty in general. Firstly, in Evidential Deep Learning, model uncertainty usually is no longer estimated via the uncertainty in learnable model parameters, but instead through the parameters of the prior or posterior distribution. Furthermore, distinguishing epistemic from distributional uncertainty allows us to differentiate uncertainty due to underspecification from uncertainty due to a lack of evidence. In BMA, these notions are indistinguishable: In theory, model uncertainty on OOD data should be high since the model is underspecified on them, however theoretical and empirical work have shown this is not always the case (Ulmer et al., 2020; Ulmer & Cinà, 2021; Van Landeghem et al., 2022). Even then, the additive decomposition of the mutual information has been critized since the model will also have a lot of *uncertainty about its aleatoric uncertainty* in the beginning of the training process (Hüllermeier, 2022). Furthermore, even when we obtain the best possible model within its hypothesis class, using the discussed methods it is impossible to estimate uncertainty induced by a misspecified hypothesis class. This can motivate approaches in which auxiliary models directly predict model uncertainty (Jain et al., 2021; Zerva et al., 2022).

3.4 Existing Approaches for Dirichlet Networks

Being able to quantify aleatoric, epistemic and distributional uncertainty in a single forward pass and in closed form are desirable traits, as they simplify the process of obtaining different uncertainty scores. However, it is important to note that the behavior of the Dirichlet distributions in Figure 4 are idealized. In the usual way of training neural networks through empirical risk minimization, Dirichlet networks are not incentivized to behave in the depicted way. Thus, when comparing existing approaches for parameterizing Dirichlet priors in Section 3.4.1 and posteriors in Section 3.4.2,[6] we mainly focus on the different ways in which authors try to tackle this problem by means of loss functions and training procedures. We give an overview over the discussed works in Tables 1 and 2 in these respective sections. For additional details, we refer the reader to Appendix C for general derivations concerning the Dirichlet distribution. We dedicate Appendix D to derivations of the different loss functions and regularizers and give a detailed overview over their mathematical forms in Appendix E. Available code repositories for all works surveyed are listed in Appendix A.2.

3.4.1 Prior Networks

The key challenge in training Dirichlet networks is to ensure both high classification performance and the intended behavior under foreign data inputs. For this reason, most discussed works follow a loss function design using two parts: One optimizing for task accuracy to achieve the former goal, the other optimizing for a flat Dirichlet distribution, as flatness suggests a lack of evidence. To enforce flatness, the predicted Dirichlet is compared to a uniform distribution using some probabilistic divergence measure. We divide prior networks into two groups: Approaches using additional OOD data for this purpose (*OOD-dependent approaches*), and those which do not required OOD data (*OOD-free approaches*), as listed in Table 1.

OOD-free approaches Apart from a standard negative log-likelihood loss (NLL) as used by Haussmann et al. (2019), one simple approach to optimizing the model is to impose a l_p-loss between the one-hot encoding $\mathbf{y}$ of the original label y and the categorical distribution $\boldsymbol{\mu}$. Tsiligkaridis (2019) show that since the values of $\boldsymbol{\mu}$ depend directly on the predicted concentration parameters $\boldsymbol{\alpha}$, a generalized loss can be derived to be upper-bounded by the following expression (see the full derivation is given in Appendix D.3):

$$\mathbb{E}_{p(\boldsymbol{\mu}|\,\mathbf{x},\boldsymbol{\theta})}\left[||\,\mathbf{y}-\boldsymbol{\mu}||_p\right] \leq \left(\frac{\Gamma(\alpha_0)}{\Gamma(\alpha_0+p)}\right)^{\frac{1}{p}} \left(\frac{\Gamma\left(\sum_{k\neq y}\alpha_k+p\right)}{\Gamma\left(\sum_{k\neq y}\alpha_k\right)} + \sum_{k\neq y}\frac{\Gamma(\alpha_k+p)}{\Gamma(\alpha_k)}\right)^{\frac{1}{p}} \tag{15}$$

[6]Even though the term *prior* and *posterior network* were coined by Malinin & Gales (2018) and Charpentier et al. (2020) for their respective approaches, we use them in the following as an umbrella term for all methods targeting a prior or posterior distribution.

Table 1: Overview over prior networks for classification. $(*)$ OOD samples were created inspired by the approach of Liang et al. (2018). ID: Using in-distribution data samples.

Method	Loss function	Architecture	OOD-free training?
Prior network (Malinin & Gales, 2018)	ID KL w.r.t smoothed label & OOD KL w.r.t. uniform prior	MLP / CNN	✗
Prior networks (Malinin & Gales, 2019)	Reverse KL of Malinin & Gales (2018)	CNN	✗
Information Robust Dirichlet Networks (Tsiligkaridis, 2019)	l_p norm w.r.t one-hot label & Approx. Rényi divergence w.r.t. uniform prior	CNN	✓
Dirichlet via Function Decomposition (Biloš et al., 2019)	Uncertainty Cross-entropy & mean & variance regularizer	RNN	✓
Prior network with PAC Regularization (Haussmann et al., 2019)	Negative log-likelihood loss + PAC regularizer	BNN	✓
Ensemble Distribution Distillation (Malinin et al., 2020b)	Knowledge distillation objective	MLP / CNN	✓
Self-Distribution Distillation (Fathullah & Gales, 2022)	Knowledge distillation objective	CNN	✓
Prior networks with representation gap (Nandy et al., 2020)	ID & OOD Cross-entropy + precision regularizer	MLP / CNN	✗
Prior RNN (Shen et al., 2020)	Cross-entropy + entropy regularizer	RNN	(✗)*
Graph-based Kernel Dirichlet distribution estimation (GKDE) (Zhao et al., 2020)	l_2 norm w.r.t. one-hot label & KL reg. with node-level distance prior & Knowledge distillation objective	GNN	✓

Since the sum over concentration parameters excludes the one corresponding to the gold label, this loss can be seen as reducing the density on the areas of the probability simplex that do not correspond to the target class. Sensoy et al. (2018) specifically utilize the l_2 loss, which has the following form (see Appendix D.4):

$$\mathbb{E}_{p(\boldsymbol{\mu}|\,\mathbf{x},\boldsymbol{\theta})}\Big[||\,\mathbf{y}-\boldsymbol{\mu}||_2^2\Big] = \sum_{k=1}^{K}\Big(\mathbf{1}_{y=k}-\frac{\alpha_k}{\alpha_0}\Big)^2 + \frac{\alpha_k(\alpha_0-\alpha_k)}{\alpha_0^2(\alpha_0+1)} \tag{16}$$

where $\mathbf{1}_{(\cdot)}$ denotes the indicator function. Since $\alpha_k/\alpha_0 \leq 1$, we can see that the term with the indicator functions penalizes the network when the concentration parameter α_k corresponding to the correct label does not exceed the others. The remaining aspect lies in the regularization: To achieve reliable predictive uncertainty, the density associated with incorrect classes should be reduced. One such option is to decrease the Kullback-Leibler divergence from a uniform Dirichlet (see Appendix C.3):

$$\mathrm{KL}\Big[p(\boldsymbol{\mu}|\boldsymbol{\alpha})\Big|\Big|p(\boldsymbol{\mu}|\mathbf{1})\Big] = \log\frac{\Gamma(K)}{B(\boldsymbol{\alpha})} + \sum_{k=1}^{K}(\alpha_k-1)\big(\psi(\alpha_k)-\psi(\alpha_0)\big) \tag{17}$$

In the case of Zhao et al. (2020), who apply their model to graph structures, they do not decrease the divergence from a uniform Dirichlet, but incorporate information about the local graph neighborhood into the reference distribution by considering the distance from and label of close nodes.[7] Nevertheless, the KL-divergence w.r.t. a uniform Dirichlet is used by many of the following works. Other divergence measures

[7] They also add another knowledge distillation term (Hinton et al., 2015) to their loss, for which the model tries to imitate the predictions of a vanilla Graph Neural Network that functions as the teacher network.

are also possible: Tsiligkaridis (2019) instead use a local approximation of the Rényi divergence.[8] First, the concentration parameter for the correct class α_y is removed from the Dirichlet by creating $\tilde{\boldsymbol{\alpha}} = (1-\mathbf{y})\cdot\boldsymbol{\alpha}+\mathbf{y}$. Then, the remaining concentration parameters are pushed towards uniformity by the divergence measure, which can be derived to be

$$\text{Rényi}\Big[p(\boldsymbol{\mu}|\tilde{\boldsymbol{\alpha}})\Big|\Big|p(\boldsymbol{\mu}|\mathbf{1})\Big] \approx \frac{1}{2}\Big[\sum_{k\neq y}\big(\alpha_k-1\big)^2\big(\psi^{(1)}(\alpha_j)-\psi^{(1)}(\tilde{\alpha}_0)\big)-\psi^{(1)}(\tilde{\alpha}_0)\sum_{\substack{k\neq k'\\ k\neq y,\ k'\neq y}}\big(\alpha_k-1\big)\big(\alpha_{k'}-1\big)\Big] \quad (18)$$

where $\psi^{(1)}$ denotes the first-order polygamma function, defined as $\psi^{(1)}(x) = \frac{d}{dx}\psi(x)$. Since the sums ignore the concentration parameter of the correct class, only the ones of the incorrect classes are penalized. Haussmann et al. (2019) derive an entirely different regularizer using Probably Approximately Correct (PAC) bounds from learning theory, that together with the negative log-likelihood gives a proven bound to the expected true risk of the classifier. Setting a scalar δ allows one to set the desired risk, i.e. the model's expected risk is guaranteed to be the same or less than the derived PAC bound with a probability of $1-\delta$. For a problem with N available training data points, the following *upper bound* is presented:

$$\sqrt{\frac{\text{KL}\big[p(\boldsymbol{\mu}|\boldsymbol{\alpha})\big|\big|p(\boldsymbol{\mu}|\mathbf{1})\big]-\log\delta}{N}-1}. \quad (19)$$

This upper bound is then used as the actual regularizer term in practice. We see that even from the learning-theoretic perspective, this method follows the intuition of the original KL regularizer in a shifted and scaled form. Haussmann et al. (2019) also admit that in this form, the regularizer does not allow for a direct PAC interpretation anymore, since its approximates only admits a loose bound on the risk. Yet, they demonstrate its usefulness in their experiments. Summarizing all of the presented approaches thus far, we can see that they try to force the to model to concentrate the Dirichlet's density solely on the parameter corresponding to the right label—expecting a more flat density for difficult or unknown inputs.

Knowledge distillation A way to avoid the use of OOD examples while still using external information for regularization is to use *knowledge distillation* (Hinton et al., 2015). Here, the core idea lies in a student model learning to imitate the predictions of a more complex teacher model. Malinin et al. (2020b) exploit this idea and show that prior networks can also be distilled using an ensemble of classifiers and their predicted categorical distributions (akin to learning Figure 4e from Figure 4a), which does not require regularization at all, but comes at the cost of having to train an entire ensemble a priori. Trying to solve this shortcoming, Fathullah & Gales (2022) propose to use a shared feature extractor between the student and the teacher network. Instead of training an ensemble, diverse predictions are obtained from the teacher network through the use of Gaussian dropout, which are distilled into a Dirichlet distribution as in Malinin et al. (2020b).

OOD-dependent approaches A uniform Dirichlet in the face of unknown inputs can also be achieved explicitly by training with OOD inputs and learning to be uncertain on them. We discuss a series of works utilizing this direction next. Malinin & Gales (2018) simply minimize the KL divergence to a uniform Dirichlet on OOD data points. This way, the model is encouraged to be agnostic about its prediction in the face of unknown inputs. Further, instead of an l_p norm, they utilize another KL term to train the model on predicting the correct label, minimizing the distance between the predicted concentration parameters and the gold label. However, since only a gold *label* and not a gold *distribution* is available, they create one by re-distributing some of the density from the correct class onto the rest of the simplex (see Appendix E for full form). In their follow-up work, Malinin & Gales (2019) argue that the asymmetry of the KL divergence as the main objective creates undesirable properties in producing the correct behavior of the predicted Dirichlet, since it creates a multi- instead of unimodal target distribution. They therefore propose to use the reverse KL instead (see Appendix D.5 for the derivation), which enforces the desired unimodal target. Nandy

[8]The Kullback-Leibler divergence can be seen as a special case of the Rényi divergence (van Erven & Harremoës, 2014), where the latter has a stronger information-theoretic underpinning.

et al. (2020) refine this idea further, stating that even with reverse KL training high epistemic and high distributional uncertainty (Figures 4d and 4e) might be confused, and instead propose novel loss functions producing a *representation gap* (Figure 4f), which aims to be more easily distinguishable. In this case, spread out densities signify epistemic uncertainty, whereas densities concentrated entirely on the edges of the simplex indicate distributional uncertainty. The way they achieve this goal is two-fold: In addition to minimizing the negativ log-likelihood loss on in-domain and maximizing the entropy on OOD examples, they also penalize the precision of the Dirichlet (see Appendix E for full form). Maximizing the entropy on OOD examples hereby serves the same function as minimizing the KL w.r.t. to a uniform distribution, and can be implemented using the closed-form solution in Appendix C.2:

$$H\big[p(\boldsymbol{\mu}|\,\boldsymbol{\alpha})\big] = \log B(\boldsymbol{\alpha}) + (\alpha_0 - K)\psi(\alpha_0) - \sum_{k=1}^{K}(\alpha_k - 1)\psi(\alpha_k) \tag{20}$$

Sequential models We also have identified two sequential applications of prior networks in the literature: For Natural Language Processing, Shen et al. (2020) train a recurrent neural network for spoken language understanding using a simple cross-entropy loss. Instead of using OOD examples for training, they maximize the entropy of the model on data inputs given a learned, noisy version of the predicted concentration parameters. In comparison, Biloš et al. (2019) apply their model to asynchronous event classification and note that the standard cross-entropy loss only involves a point estimate of a categorical distribution, discarding all the information contained in the predicted Dirichlet. For this reason, they propose an *uncertainty-aware* cross-entropy (UCE) loss instead, which has a closed-form solution in the Dirichlet case (see Appendix D.6)

$$\mathcal{L}_{\text{UCE}} = \psi(\alpha_y) - \psi(\alpha_0), \tag{21}$$

with ψ referring to the digamma function. By mimizing the difference between the digamma values of α_y and α_0, the model learns to concentrate density on the correct class. Since their final concentration parameters are created using additional information from a class-specific Gaussian process, they further regularize the mean and variance for OOD data points using an extra loss term, incentivizing a loss mean and a variance corresponding to a pre-defined hyperparameter.

3.4.2 Posterior Networks

As elaborated on in Section 3.1, choosing a Dirichlet prior, due to its conjugacy to the categorical distribution, induces a Dirichlet posterior distribution. Like the prior before, surveyed works listed in Table 2 parameterize the posterior with a neural network. The challenges hereby are two-fold: Accounting for the number of class observations N_k that make up part of the posterior density parameters $\boldsymbol{\beta}$ (Equation (10)), and, similarly to prior networks, ensuring the wanted behavior on the probability simplex for in- and out-of-distribution inputs. Sensoy et al. (2018) base their approach on the Dempster-Shafer theory of evidence (Yager & Liu, 2008; lending its name to the term "Evidential Deep Learning") and its formalization via subjective logic (Audun, 2018), where subjective beliefs about probabilities are expressed through Dirichlet distributions. In doing so, an agnostic belief in form of a uniform Dirichlet prior $\forall k : \alpha_k = 1$ is updated using pseudo-counts N_k, which are predicted by a neural network. This is different from prior networks, where the prior concentration parameters $\boldsymbol{\alpha}$ are predicted instead. In both cases, this does not require any modification to a model's architecture except for replacing the softmax output function by a ReLU (or similar). Sensoy et al. (2018) for instance train their model using the same techniques presented in the previous section: The main objective is the l_2 loss, penalizing the difference between the predicted Dirichlet and the one-hot encoded class label (Appendix D.4), and the KL divergence from a uniform Dirichlet is used for regularization.

Generating OOD samples using generative models Since OOD examples are not always readily available, several works try to create artificial samples using deep generative models. Hu et al. (2021) train a Wasserstein GAN (Arjovsky et al., 2017) to generate OOD samples, on which the network's uncertainty is maximized. The uncertainty is given through *vacuity*, defined as $K/\sum_k \beta_k$. The vacuity compares a uniform prior belief against the amassed evidence $\sum_k \beta_k$, an thus is 1 when there is no additonal evidence available.

Table 2: Overview over posterior networks for classification. OOD data is created using (†) the fast-sign gradient method (Kurakin et al., 2017), a (‡) Variational Auto-Encoder (VAE; Kingma & Welling, 2014) or (§) a Wasserstein GAN (WGAN; Arjovsky et al., 2017). NLL: Negative log-likelihood. CE: Cross-entropy.

Method	Loss function	Architecture	OOD-free training?
Evidential Deep Learning (Sensoy et al., 2018)	l_2 norm w.r.t. one-hot label + KL w.r.t. uniform prior	CNN	✓
Regularized ENN (Zhao et al., 2019)	l_2 norm w.r.t. one-hot label + Uncertainty regularizer on OOD/ difficult samples	MLP / CNN	✗
WGAN–ENN (Hu et al., 2021)	l_2 norm w.r.t. one-hot label + Uncertainty regularizer on synth. OOD	MLP / CNN + WGAN	(✗)§
Variational Dirichlet (Chen et al., 2018)	ELBO + Contrastive Adversarial Loss	CNN	(✗)†
Dirichlet Meta-Model (Shen et al., 2022)	ELBO + KL w.r.t. uniform prior	CNN	✓
Belief Matching (Joo et al., 2020)	ELBO	CNN	✓
Posterior Networks (Charpentier et al., 2020)	Uncertainty CE (Biloš et al., 2019) + Entropy regularizer	MLP / CNN + Norm. Flow	✓
Graph Posterior Networks (Stadler et al., 2021)	Same as Charpentier et al. (2020)	GNN	✓
Generative Evidential Neural Networks (Sensoy et al., 2020)	Contrastive NLL + KL between uniform & Dirichlet of wrong classes	CNN	(✗)‡

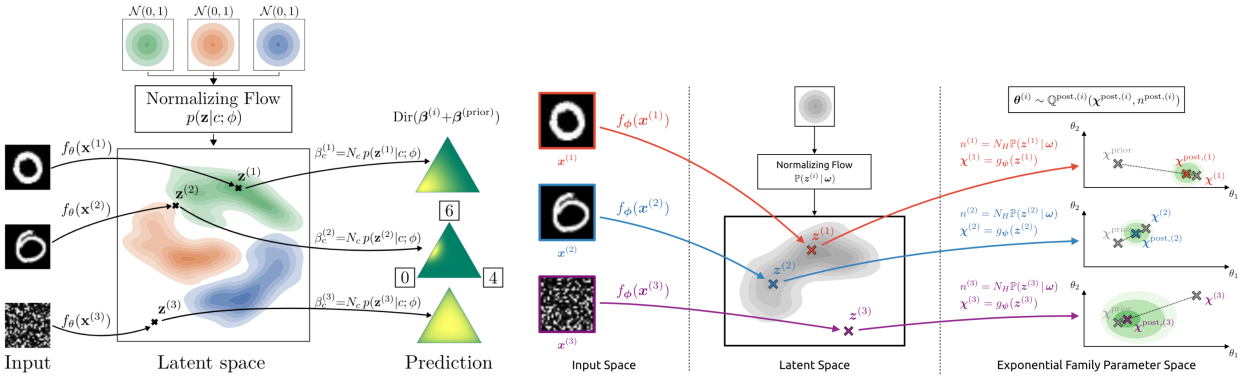

(a) Posterior Network (Charpentier et al., 2020).

(b) Natural Posterior Network (Charpentier et al., 2022).

Figure 5: Schematic of the Posterior Network and Natural Posterior Network, taken from Charpentier et al. (2020; 2022), respectively. In both cases, an encoder $f_{\boldsymbol{\theta}}$ maps inputs to a latent representation $\mathbf{z}$. NFs then model the latent densities, which are used together with the prior concentration to produce the posterior parameters. In (a), the latent representation of $\mathbf{x}^{(1)}$ lies right in the modelled density of the first class, and thus receives a confident prediction. The latent $\mathbf{z}^{(2)}$ lies between densities, creating aleatoric uncertainty. $\mathbf{x}^{(3)}$ is an OOD input, is mapped to a low-density area of the latent space and thus produces an uncertain prediction. The differences in the two approaches is that the Posterior Network in (a) uses one NF per class, while only one NF is used in (b). Furthermore, (b) constitutes a generalization to different exponential family distributions, and is not restricted to classification problems (see main text for more detail).

In a follow-up work, Sensoy et al. (2020) similarly train a model using a contrastive loss with artificial OOD samples from a Variational Autoencoder (Kingma & Welling, 2014), and a KL-based regularizer similar to that of Tsiligkaridis (2019), where the density for posterior concentration parameters β_k that do not correspond to the gold label are pushed to the uniform distribution.

Posterior networks via Normalizing Flows Charpentier et al. (2020) also set $\boldsymbol{\alpha}$ to a uniform prior, but obtain the pseudo-observations N_k in a different way: Instead of a model predicting them directly, N_k is determined by the number of examples of a certain class in the training set. This quantity is further modified in the following way: An encoder model $f_{\boldsymbol{\theta}}$ produces a latent representation $\mathbf{z}$ of some input. A (class-specific) normalizing flow[9] (NF; Rezende & Mohamed, 2015) with parameters $\boldsymbol{\phi}$ then assigns a probability to this latent representation, which is used to weight N_k:

$$\beta_k = \alpha_k + N_k \cdot p(\mathbf{z} \,|y = k, \boldsymbol{\phi}); \quad \mathbf{z} = f_{\boldsymbol{\theta}}(\mathbf{x}). \tag{22}$$

This has the advantage of producing low probabilities for strange inputs like the noise as depicted in Figure 5a, which in turn translate to low concentration parameters of the posterior Dirichlet, as it falls back onto the uniform prior. The model is optimized using the same uncertainty-aware cross-entropy loss as in Biloš et al. (2019) with an additional entropy regularizer, encouraging density only around the correct class. This scheme is also applied to Graph Neural Networks by Stadler et al. (2021): In order to take the neighborhood structure of the graph into account, the authors also use a Personalized Page Rank scheme to diffuse node-specific posterior parameters $\boldsymbol{\beta}$ between neighboring nodes. The Page Rank scores, reflecting the importance of a neighboring node to the current node, can be approximated using power iteration (Klicpera et al., 2019) and used to aggregate the originally predicted concentration parameters $\boldsymbol{\beta}$ on a per-node basis.

A generalization of the posterior network method to exponential family distributions is given by Charpentier et al. (2022). Akin to the update for the posterior Dirichlet parameters, the authors formulate a general Bayesian update rule as

$$\boldsymbol{\chi}_i^{\text{post}} = \frac{n^{\text{prior}} \boldsymbol{\chi}^{\text{prior}} + n_i \boldsymbol{\chi}_i}{n^{\text{prior}} + n_i}; \quad \mathbf{z}_i = f_{\boldsymbol{\theta}}(\mathbf{x}_i); \quad n_i = N \cdot p(\mathbf{z} \,|\boldsymbol{\phi}); \quad \boldsymbol{\chi}_i = g_{\boldsymbol{\psi}}(\mathbf{x}_i). \tag{23}$$

$\boldsymbol{\chi}$ here denotes the parameters of the exponential family distribution and n the evidence. Thus, posterior parameters for a sample $\mathbf{x}_i$ are obtained by updating the prior parameter and some prior evidence by some input-dependent pseudo-evidence n_i and parameters $\boldsymbol{\chi}_i$: Again, given a latent representation by an encoder $\mathbf{z}$, a (this time single) normalizing flow predicts $n_i = N_H \cdot p(\mathbf{z} \,|\boldsymbol{\phi})$ based on some pre-defined certainty budget N_H.[10] The update parameters $\boldsymbol{\chi}_i$ are predicted by an additional network $\boldsymbol{\chi}_i = g_{\boldsymbol{\psi}}(\mathbf{z})$, see Figure 5b. For classification, $n^{\text{prior}} = 1$ and $\boldsymbol{\chi}^{\text{prior}}$ corresponds to the uniform Dirichlet, while $\boldsymbol{\chi}_i$ are concentration parameters predicted by an output layer based on the latent encoding. For unfamiliar inputs, this method will again result in a small pseudo-evidence term n_i, reflecting high model uncertainty. Since the generalization to the exponential family implies the application of this scheme to normal distributions, we will discuss the same method applied to regression in the next section.

Posterior networks via variational inference Another route lies in directly parameterizing the posterior parameters $\boldsymbol{\beta}$. Given a target distribution defined by a uniform Dirichlet prior plus the number of times an input is associated with a specific label, Chen et al. (2018) optimize a distribution matching objective, i.e. the KL-divergence between the posterior parameters predicted by a neural network and the target distribution. Since this objective is intractable to optimize directly, this leaves us to instead model an *approximate posterior* using variational inference methods. As the KL divergence between the true and approximate posterior is infeasible to estimate, variational methods usually optimize the *evidence lower bound* (ELBO):

[9] A NF is a generative model, estimating a density in the feature space by mapping it to a Gaussian in a latent space by a series of invertible, bijective transformations. The probability of an input can then be estimated by calculating the probability of its latent encoding under that Gaussian and applying the change-of-variable formula, traversing the flow in reverse. Instead of mapping from the feature space into latent space, the flows in Charpentier et al. (2020) map from the encoder latent space into a separate, second latent space.

[10] The certainty budget can simply be set to the number of available datapoints, however Charpentier et al. (2022) suggest to set it to $\log N_H = \frac{1}{2}\Big(H \log(2\pi) + \log(H+1)\Big)$ to better scale with the dimensionality H of the latent space.

Table 3: Overview over Evidential Deep Learning methods for regression.

Method	Parameterized distribution	Loss function	Model
Deep Evidential Regression (Amini et al., 2020)	Normal-Inverse Gamma Prior	Negative log-likelihood loss + KL w.r.t. uniform prior	MLP / CNN
Deep Evidential Regression with Multi-task Learning (Oh & Shin, 2022)	Normal-Inverse Gamma Prior	Like Amini et al. (2020), with additional Lipschitz-modified MSE loss	MLP / CNN
Multivariate Deep Evidential Regression (Meinert & Lavin, 2021)	Normal-Inverse Wishart Prior	Like Amini et al. (2020), but tying two predicted params. instead of using a regularizer	MLP
Regression Prior Network (Malinin et al., 2020a)	Normal-Wishart Prior	Reverse KL (Malinin & Gales, 2019)	MLP / CNN
Natural Posterior Network (Charpentier et al., 2022)	Inverse-χ^2 Posterior	Uncertainty Cross-entropy (Biloš et al., 2019) + Entropy regularizer	MLP / CNN + Norm. Flow

$$\mathcal{L}_{\text{ELBO}} = \underbrace{\psi(\beta_y) - \psi(\beta_0)}_{\text{UCE loss}} \underbrace{- \log \frac{B(\boldsymbol{\beta})}{B(\boldsymbol{\gamma})} + \sum_{k=1}^{K} (\beta_k - \gamma_k)\big(\psi(\beta_k) - \psi(\beta_0)\big)}_{\text{KL-divergence}} \tag{24}$$

in which we can identify to consist of the uncertainty-aware cross-entropy (UCE) loss used by Biloš et al. (2019); Charpentier et al. (2020; 2022) and the KL-divergence between two Dirichlets (Appendix C.3). This approach is also employed by Joo et al. (2020), Chen et al. (2018) and Shen et al. (2022), while the latter predict posterior parameters based on the activations of different layers of a pre-trained feature extractor.

4 Evidential Deep Learning for Regression

Because the EDL framework provides convenient uncertainty estimation, the question naturally arises of whether it can be extended to regression problems as well. The answer is affirmative, although the Dirichlet distribution is not an appropriate choice in this case. It is very common to model a regression problem using a normal likelihood (Bishop, 2006; Chapter 3.3). As such, there are multiple potential choices for a prior distribution. The methods listed in Table 3 either choose the Normal-Inverse Gamma distribution (Amini et al., 2020; Charpentier et al., 2022), inducing a scaled inverse-χ^2 posterior (Gelman et al., 1995),[11] or a Normal-Wishart prior (Malinin et al., 2020a). We will discuss these approaches in turn.

Univariate regression Amini et al. (2020) model the regression problem as a normal distribution with unknown mean and variance $\mathcal{N}(y; \mu, \sigma^2)$, and use a normal prior for the mean with $\mu \sim \mathcal{N}(\gamma, \sigma^2\nu^{-1})$ and an inverse Gamma prior for the variance with $\sigma^2 \sim \Gamma^{-1}(\alpha, \beta)$, resulting in a combined Inverse-Gamma prior with parameters $\gamma, \nu, \alpha, \beta$, shown in Figure 6. These are predicted by different "heads" of a neural network. For predictions, the expectation of the mean corresponds to $\mathbb{E}[\mu] = \gamma$, and aleatoric and epistemic uncertainty can then be estimated using the expected value of the variance as well as the variance of the mean, respectively, which have closed form solutions under this parameterization:

$$\mathbb{E}[\sigma^2] = \frac{\beta}{\alpha - 1}; \quad \text{Var}[\mu] = \frac{\beta}{\nu(\alpha - 1)} \tag{25}$$

By choosing to optimize using a negative log-likelihood objective, we can actually evaluate the loss function analytically, since the likelihood function corresponds to a Student's t-distribution with γ degrees of freedom, mean $\beta(1 + \nu)/(\nu\alpha)$ and 2α variance:

[11] The form of the Normal-Inverse Gamma posterior and the Normal Inverse-χ^2 posterior are interchangable using some parameter substitutions (Murphy, 2007).

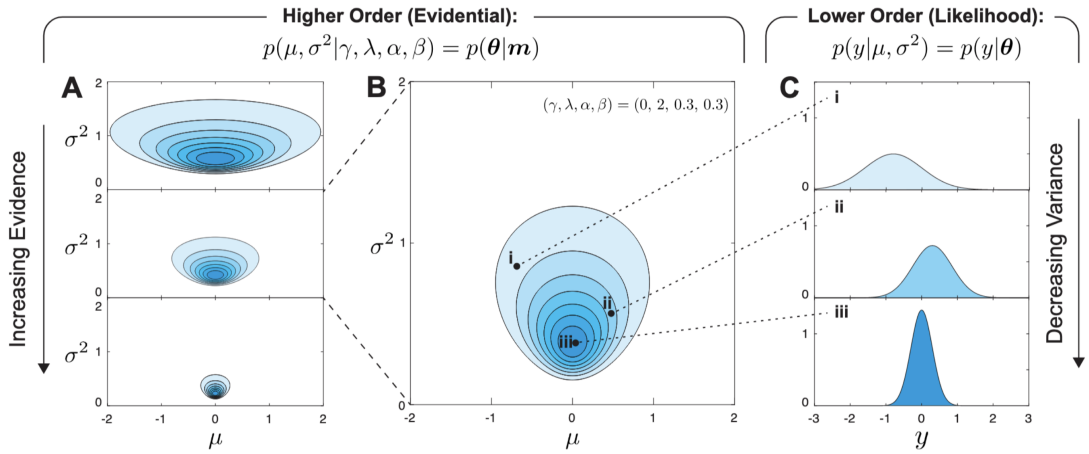

Figure 6: Example of an application of Evidential Deep Learning for regression, taken from Amini et al. (2020). The neural network predicts an Normal Inverse-Gamma prior, whose corresponding normal likelihoods display decreasing variance (and thus uncertainty) in the face of stronger evidence.

$$\mathcal{L}_{\text{NLL}} = \frac{1}{2}\log\left(\frac{\pi}{\nu}\right) - \alpha\log\Omega + \left(\alpha + \frac{1}{2}\right)\log\left((y_i - \gamma)^2\nu + \Omega\right) + \log\left(\frac{\Gamma(\alpha)}{\Gamma(\alpha + \frac{1}{2})}\right) \tag{26}$$

using $\Omega = 2\beta(1 + \nu)$. Akin to the entropy regularizer for Dirichlet networks, Amini et al. (2020) propose a regularization term that only allows for concentrating density on the correct prediction:

$$\mathcal{L}_{\text{reg}} = |y_i - \gamma| \cdot (2\nu + \alpha) \tag{27}$$

Since $\mathbb{E}[\mu] = \gamma$ is the prediction of the network, the second term in the product will be scaled by the degree to which the current prediction deviates from the target value. Since ν and α control the variance of the mean and the variance of the normal likelihood, this term encourages the network to decrease the evidence for mispredicted data samples. As Amini et al. (2020) point out, large amounts of evidence are not punished in cases where the prediction is close to the target. However, Oh & Shin (2022) argue that this combination of objectives might create adverse incentives for the model during training: Since the difference between the prediction and target in Equation (26) is scaled by ν, the model could learn to increase the predictive uncertainty by decreasing ν instead of improving its prediction. They propose to ameliorate this issue by using a third loss term of the form

$$\mathcal{L}_{\text{MSE}} = \begin{cases} (y_i - \gamma)^2 & \text{if } (y_i - \gamma)^2 < U_{\nu,\alpha} \\ 2\sqrt{U_{\nu,\alpha}}|y_i - \gamma| - U_{\nu,\alpha} & \text{if } (y_i - \gamma)^2 \geq U_{\nu,\alpha} \end{cases} \tag{28}$$

where $U_{\nu,\alpha} = \min(U_\nu, U_\alpha)$ denotes the minimum value for the uncertainty thresholds for ν, α given over a mini-batch, which are themselves defined as

$$U_\nu = \frac{\beta(\nu + 1)}{\alpha\nu}; \quad U_\alpha = \frac{2\beta(\nu + 1)}{\nu}\left[\exp\left(\psi\left(\alpha + \frac{1}{2}\right) - \psi(\alpha)\right) - 1\right]. \tag{29}$$

These expression are obtained by taking the derivatives $\partial\mathcal{L}_{\text{NLL}}/\partial\nu$, $\partial\mathcal{L}_{\text{NLL}}/\partial\alpha$ and solving for the parameters, thus giving us the values for ν and α for which the loss gradients are maximal. In combination with Equation (28), Equation (29) ensures that, should the model error exceed $U_{\nu,\alpha}$, the error is rescale. Thus, this rescaling bounds the Lipschitz constant of the loss function, motivating the model to ensure the correctness of its prediction, since its ability to increase uncertainty to decrease its loss is now limited.

Posterior networks for regression Another approach for regression is the Natural Posterior Network by Charpentier et al. (2022), which was already discussed for classification in Section 3.4.2. But since the proposed approach is a generalization for exponential family distributions, it can be applied to regression as well, using a Normal likelihood and Normal Inverse-Gamma prior. The Bayesian update rule in Equation (23) is adapted as follows: n is set to $n = \lambda = 2\alpha$, and $\boldsymbol{\chi} = \left[\mu_0 \mid \mu_0^2 + 2\beta/n\right]^T$. Feeding an input into the natural posterior network again first produces a latent encoding $\mathbf{z}$, from which a NF predicts $n_i = N_H \cdot p(\mathbf{z} \,|\boldsymbol{\phi})$, and an additional network produces $\boldsymbol{\chi}_i = g_{\boldsymbol{\psi}}(\mathbf{z})$, which are used in Equation (23) to produce $\boldsymbol{\chi}^{\text{post}}$ and n^{post}, from which the parameters of the posterior Normal Inverse-Gamma can be derived. The authors also produce a general exponential family form of the UCE loss by Biloš et al. (2019), consisting of expected log-likelihood and an entropy regularizer, which they derive for the regression parameterization. Again, this approach relies on the density estimation capabilities of the NF to produce an agnostic belief about the right prediction for OOD examples (see Figure 5b).

Multivariate evidential regression There are also some works offering solutions for multivariate regression problems: Malinin et al. (2020a) can be seen as a multivariate generalization of the work of Amini et al. (2020), where a combined Normal-Wishart prior is formed to fit the now Multivariate Normal likelihood. Again, the prior parameters are the output of a neural network, and uncertainty can be quantified in a similar way. For training purposes, they apply two different training objectives using the equivalent of the reverse KL objective of Malinin & Gales (2019) as well as of the knowledge distillation objective of Malinin et al. (2020b), which does not require OOD data for regularization purposes. Meinert & Lavin (2021) also provide a solution using a Normal Inverse-Wishart prior. In a similar vein to Oh & Shin (2022), they argue that the original objective proposed by Amini et al. (2020) can be minimized by increasing the network's uncertainty instead of the decreasing the mismatch of its prediction. As a solution, they simply propose to tie β and ν via a hyperparameter.

5 Related Work

Other Approaches to Uncertainty Quantification The need for the quantification of uncertainty in order to earn the trust of end-users and stakeholders has been a key driver for research (Bhatt et al., 2021; Jacovi et al., 2021; Liao & Sundar, 2022). Existing methods can broadly be divided into frequentist and Bayesian methods, where the former judge the confidence of a model based on its predicted probabilities. Unfortunately, standard neural discriminator architectures have been proven to possess unwanted theoretical properties w.r.t. OOD inputs (Hein et al., 2019; Ulmer & Cinà, 2021) and might therefore be unable to detect potentially risky inputs.[12] Further, a large line of research works has questioned the calibration of models (Guo et al., 2017; Nixon et al., 2019; Desai & Durrett, 2020; Minderer et al., 2021; Wang et al., 2021b), i.e. to what extend the probability score of a class—also referred to as its confidence—corresponds to the chance of a correct prediction. Instead of relying on the confidence score alone, another way lies in constructing prediction sets consisting of the classes accumulating a certain share of the total predictive mass (Kompa et al., 2021; Ulmer et al., 2022). By scoring a held-out population of data points to calibrate these prediction sets, we can also obtain frequentist guarantees in a procedure referred to a *conformal prediction* (Papadopoulos et al., 2002; Vovk et al., 2005; Lei & Wasserman, 2014; Angelopoulos & Bates, 2021). This however still does not let us distinguish different notions of uncertainty. A popular *Bayesian* way to overcome this blemish by aggregating multiple predictions by networks in the Bayesian model averaging framework (Mackay, 1992; MacKay, 1995; Hinton & Van Camp, 1993; Neal, 2012; Jeffreys, 1998; Wilson & Izmailov, 2020; Kristiadi et al., 2020; Daxberger et al., 2021; Gal & Ghahramani, 2016; Blundell et al., 2015; Lakshminarayanan et al., 2017). Nevertheless, many of these methods have been shown not to produce diverse predictions (Wilson & Izmailov, 2020; Fort et al., 2019) and to deliver subpar performance and potentially misleading uncertainty estimates under distributional shift (Ovadia et al., 2019; Masegosa, 2020; Wenzel et al., 2020; Izmailov et al., 2021a;b), raising doubts about their efficacy.

[12] Pearce et al. (2021) argue that some insights might partially be mislead by low-dimensional intuitions, and that empirically OOD data in higher dimensions tend to be mapped into regions of higher uncertainty.

Related Approaches to EDL Kull et al. (2019) found an appealing use of the Dirichlet distribution as a post-training calibration map. The proposed Posterior Network (Charpentier et al., 2020; 2022) can furthermore be seen as related to another, competing approach, namely the combination of neural discriminators with density estimation methods, for instance in the form of energy-based models (Grathwohl et al.; Elflein et al., 2021) or other hybrid architectures (Lee et al., 2018; Mukhoti et al., 2021).

Applications of EDL Some of the discussed models have already found a variety of applications, such as in autonomous driving (Capellier et al., 2019; Liu et al., 2021; Petek et al., 2022; Wang et al., 2021a), remote sensing (Gawlikowski et al., 2022), medical screening (Ghesu et al., 2019; Gu et al., 2021; Li et al., 2022), molecular analysis (Soleimany et al., 2021), open set recognition (Bao et al., 2021), active learning (Hemmer et al., 2022) and model selection (Radev et al., 2021).

6 Discussion

Challenges Despite their advantages, the last chapters have pointed out key weaknesses of Dirichlet networks as well: In order to achieve the right behavior of the distribution and thus guarantee sensible uncertainty estimates (since ground truth estimates are not available), the surveyed literature proposes a variety of loss functions. Bengs et al. (2022) show formally that many of the loss functions used so far are *not* appropriate and violate basic asymptotic assumptions about epistemic uncertainty: With increasing amount of data, epistemic uncertainty should vanish, but this is not guaranteed using the commonly used loss functions. Furthermore, some approaches (Malinin & Gales, 2018; 2019; Nandy et al., 2020; Malinin et al., 2020a) require out-of-distribution data points during training. This comes with two problems: Such data is often not available or in the first place, or cannot guarantee robustness against *other* kinds of unseen OOD data, of which infinite types exist in a real-valued feature space.[13] Indeed, Kopetzki et al. (2021) found OOD detection to deteriorate across a family of EDL models under adversarial perturbation and OOD data.

Comparison to Other Approaches to Uncertainty Quantification As discussed in Section 5, several existing approaches to uncertainty quantification equally suffer from shortcomings with respect to their reliability. One possible explanation for this behavior might lie in the insight that neural networks trained in the empirical risk minimization framework tend to learn spurious but highly predictive features (Ilyas et al., 2019; Nagarajan et al., 2021). This way, inputs stemming from the training distribution can be mapped to similar parts of the latent space as data points outside the distribution even though they display (from a human perspective) blatant semantic differences, simply because these semantic features were not useful to optimize for the training objective. This can result in ID and OOD points having assigned similar feature representations by a network, a phenomenon has been coined "feature collapse" (Nalisnick et al., 2019; van Amersfoort et al., 2021; Havtorn et al., 2021). One strategy to mitigate (but not solve) this issue has been to enforce a constraint on the smoothness of the neural network function (Wei et al., 2018; van Amersfoort et al., 2020; 2021; Liu et al., 2020), thereby maintaining both a sensitivity to semantic changes in the input and robustness against adversarial inputs (Yu et al., 2019). Another approach lies in the usage of OOD data as well, sometimes dubbed "outlier exposure" (Fort et al., 2021), but displaying the same shortcomings as in the EDL case. A generally promising strategy seems to seek functional diversity through ensembling: Juneja et al. (2022) show how model instances ending up in different low-loss modes correspond to distinct generalization strategies, indicating that combining diverse strategies may lead to better generalization and thus potentially more reliable uncertainty. Attaining different solutions still creates computational overhead, despite new methods to reduce it (Garipov et al., 2018; Dusenberry et al., 2020; Benton et al., 2021).

Bayesian model averaging One of the most fundamental differences between EDL and existing approaches is the sacrifice of Bayesian model averaging (Equations (2) and (5)): In principle, combining multiple parameter estimates in supposed in a lower predictive risk (Fragoso et al., 2018). The Machine Learning community has ascribed further desiderata to this approach, such as better generalization and robustness to distributional shifts. Recent studies with exact Bayesian Neural Networks however have cast doubts on these assumptions (Izmailov et al., 2021a;b). Nevertheless, ensembles, that approximate Equation (2) via

[13] The same applies to the artificial OOD data in Chen et al. (2018); Shen et al. (2020); Sensoy et al. (2020).

Monte Carlo estimates, remain state-of-the-art on many uncertainty benchmarks. EDL abandons modelling epistemic uncertainty through the learnable parameters, and instead expresses it through the uncertainty in prior / posterior parameters. This loses functional diversity which could aid generalization, while sidestepping computational costs. Future research could therefore explore the combination of both paradigms, as proposed by Haussmann et al. (2019); Zhao et al. (2020); Charpentier et al. (2022).

7 Conclusion

This survey has given an overview over contemporary approaches for uncertainty estimation using neural networks to parameterize conjugate priors or the corresponding posteriors instead of likelihoods, called Evidential Deep Learning. We highlighted their appealing theoretical properties allowing for uncertainty estimation with minimal computational overhead, rendering them as a viable alternative to existing strategies. We also emphasized practical problems: In order to nudge models towards the desired behavior in the face of unseen or out-of-distribution samples, the design of the model architecture and loss function have to be carefully considered. Based on a summary and discussion of experimental findings in Appendix B, the entropy regularizer seems to be a sensible choice in prior networks when OOD data is not available. Combining discriminators with generative models like normalizing flows as in Charpentier et al. (2020; 2022), embedded in a sturdy Bayesian framework, also appears as an exciting direction for practical applications. In summary, we believe that recent advances show promising results for Evidential Deep Learning, making it a viable option in uncertainty estimation to improve safety and trustworthiness in Machine Learning systems.

References

Alexander Amini, Wilko Schwarting, Ava Soleimany, and Daniela Rus. Deep Evidential Regression. In *Advances in Neural Information Processing Systems 33: Annual Conference on Neural Information Processing Systems 2020, NeurIPS 2020, December 6-12, 2020, virtual*, 2020.

Christophe Andrieu, Nando de Freitas, and Arnaud Doucet. Reversible jump MCMC simulated annealing for neural networks. In Craig Boutilier and Moisés Goldszmidt (eds.), *UAI '00: Proceedings of the 16th Conference in Uncertainty in Artificial Intelligence, Stanford University, Stanford, California, USA, June 30 - July 3, 2000*, pp. 11–18. Morgan Kaufmann, 2000.

Anastasios N Angelopoulos and Stephen Bates. A gentle introduction to conformal prediction and distribution-free uncertainty quantification. *arXiv preprint arXiv:2107.07511*, 2021.

Martin Arjovsky, Soumith Chintala, and Léon Bottou. Wasserstein Generative Adversarial Networks. In *International conference on machine learning*, pp. 214–223. PMLR, 2017.

Jsang Audun. *Subjective Logic: A Formalism for Reasoning under Uncertainty*. Springer, 2018.

Wentao Bao, Qi Yu, and Yu Kong. Evidential Deep Learning for Open Set Action Recognition. In *Proceedings of the IEEE/CVF International Conference on Computer Vision*, pp. 13349–13358, 2021.

Alexei Bastidas. Tiny Imagenet Image Classification, 2017.

Viktor Bengs, Eyke Hüllermeier, and Willem Waegeman. On the Difficulty of Epistemic Uncertainty Quantification in Machine Learning: The Case of Direct Uncertainty Estimation through Loss Minimisation. *arXiv preprint arXiv:2203.06102*, 2022.

Gregory W. Benton, Wesley J. Maddox, Sanae Lotfi, and Andrew Gordon Wilson. Loss surface simplexes for mode connecting volumes and fast ensembling. In *Proceedings of the 38th International Conference on Machine Learning, ICML 2021, 18-24 July 2021, Virtual Event*, volume 139 of *Proceedings of Machine Learning Research*, pp. 769–779. PMLR, 2021.

Umang Bhatt, Javier Antorán, Yunfeng Zhang, Q. Vera Liao, Prasanna Sattigeri, Riccardo Fogliato, Gabrielle Gauthier Melançon, Ranganath Krishnan, Jason Stanley, Omesh Tickoo, Lama Nachman, Rumi Chunara, Madhulika Srikumar, Adrian Weller, and Alice Xiang. Uncertainty as a Form of Transparency:

Measuring, Communicating, and Using Uncertainty. In *AIES '21: AAAI/ACM Conference on AI, Ethics, and Society, Virtual Event, USA, May 19-21, 2021*, pp. 401–413. ACM, 2021.

Marin Biloš, Bertrand Charpentier, and Stephan Günnemann. Uncertainty on Asynchronous Time Event Prediction. In *Advances in Neural Information Processing Systems*, pp. 12851–12860, 2019.

Christopher M Bishop. Pattern Recognition. *Machine learning*, 128(9), 2006.

Charles Blundell, Julien Cornebise, Koray Kavukcuoglu, and Daan Wierstra. Weight Uncertainty in Neural Networks. *arXiv preprint arXiv:1505.05424*, 2015.

Yaroslav Bulatov. NotMNIST Dataset. *Google (Books/OCR), Tech. Rep.[Online]. Available: http://yaroslavvb. blogspot. it/2011/09/notmnist-dataset. html*, 2, 2011.

Edouard Capellier, Franck Davoine, Véronique Cherfaoui, and You Li. Evidential Deep Learning for Arbitrary LIDAR Object Classification in the Context of Autonomous Driving. In *2019 IEEE Intelligent Vehicles Symposium, IV 2019, Paris, France, June 9-12, 2019*, pp. 1304–1311. IEEE, 2019.

Bertrand Charpentier, Daniel Zügner, and Stephan Günnemann. Posterior network: Uncertainty estimation without ood samples via density-based pseudo-counts. *Advances in Neural Information Processing Systems*, 33:1356–1367, 2020.

Bertrand Charpentier, Oliver Borchert, Daniel Zügner, Simon Geisler, and Stephan Günnemann. Natural posterior network: Deep bayesian predictive uncertainty for exponential family distributions. In *The Tenth International Conference on Learning Representations, ICLR 2022, Virtual Event, April 25-29, 2022*. OpenReview.net, 2022.

Wenhu Chen, Yilin Shen, Hongxia Jin, and William Wang. A Variational Dirichlet Framework for Out-Of-Distribution Detection. *arXiv preprint arXiv:1811.07308*, 2018.

Tarin Clanuwat, Mikel Bober-Irizar, Asanobu Kitamoto, Alex Lamb, Kazuaki Yamamoto, and David Ha. Deep Learning for Classical Japanese Literature. *arXiv preprint arXiv:1812.01718*, 2018.

Andrea Coraddu, Luca Oneto, Aessandro Ghio, Stefano Savio, Davide Anguita, and Massimo Figari. Machine Learning Approaches for Improving Condition-Based Maintenance of Naval Propulsion Plants. *Proceedings of the Institution of Mechanical Engineers, Part M: Journal of Engineering for the Maritime Environment*, 230(1):136–153, 2016.

Peter I Corke. A Robotics Toolbox for MATLAB. *IEEE Robotics & Automation Magazine*, 3(1):24–32, 1996.

Paulo Cortez, António Cerdeira, Fernando Almeida, Telmo Matos, and José Reis. Modeling Wine Preferences by Data Mining from Physicochemical Properties. *Decision support systems*, 47(4):547–553, 2009.

Alice Coucke, Alaa Saade, Adrien Ball, Théodore Bluche, Alexandre Caulier, David Leroy, Clément Doumouro, Thibault Gisselbrecht, Francesco Caltagirone, Thibaut Lavril, et al. Snips Voice Platform: An Embedded Spoken Language Understanding System for Private-by-Design Voice Interfaces. *arXiv preprint arXiv:1805.10190*, 2018.

Mindy I Davis, Jeremy P Hunt, Sanna Herrgard, Pietro Ciceri, Lisa M Wodicka, Gabriel Pallares, Michael Hocker, Daniel K Treiber, and Patrick P Zarrinkar. Comprehensive Analysis of Kinase Inhibitor Selectivity. *Nature biotechnology*, 29(11):1046–1051, 2011.

Erik Daxberger, Agustinus Kristiadi, Alexander Immer, Runa Eschenhagen, Matthias Bauer, and Philipp Hennig. Laplace redux - effortless bayesian deep learning. In Marc'Aurelio Ranzato, Alina Beygelzimer, Yann N. Dauphin, Percy Liang, and Jennifer Wortman Vaughan (eds.), *Advances in Neural Information Processing Systems 34: Annual Conference on Neural Information Processing Systems 2021, NeurIPS 2021, December 6-14, 2021, virtual*, pp. 20089–20103, 2021.

João Ferdinando Gomes de Freitas. *Bayesian methods for neural networks*. PhD thesis, University of Cambridge, 2003.

Arthur P Dempster. A Generalization of Bayesian Inference. *Journal of the Royal Statistical Society: Series B (Methodological)*, 30(2):205–232, 1968.

Jia Deng, Wei Dong, Richard Socher, Li-Jia Li, Kai Li, and Li Fei-Fei. Imagenet: A Large-Scale Hierarchical Image Database. In *2009 IEEE conference on computer vision and pattern recognition*, pp. 248–255. Ieee, 2009.

Armen Der Kiureghian and Ove Ditlevsen. Aleatory or Epistemic? Does it matter? *Structural safety*, 31 (2):105–112, 2009.

Shrey Desai and Greg Durrett. Calibration of pre-trained transformers. In Bonnie Webber, Trevor Cohn, Yulan He, and Yang Liu (eds.), *Proceedings of the 2020 Conference on Empirical Methods in Natural Language Processing, EMNLP 2020, Online, November 16-20, 2020*, pp. 295–302. Association for Computational Linguistics, 2020.

Thomas G. Dietterich and Alexander Guyer. The familiarity hypothesis: Explaining the behavior of deep open set methods. *Pattern Recognit.*, 132:108931, 2022.

Dheeru Dua, Casey Graff, et al. UCI Machine Learning Repository. 2017.

Michael Dusenberry, Ghassen Jerfel, Yeming Wen, Yi-An Ma, Jasper Snoek, Katherine A. Heller, Balaji Lakshminarayanan, and Dustin Tran. Efficient and scalable bayesian neural nets with rank-1 factors. In *Proceedings of the 37th International Conference on Machine Learning, ICML 2020, 13-18 July 2020, Virtual Event*, volume 119 of *Proceedings of Machine Learning Research*, pp. 2782–2792. PMLR, 2020.

Sven Elflein, Bertrand Charpentier, Daniel Zügner, and Stephan Günnemann. On Out-of-distribution Detection with Energy-based Models. *arXiv preprint arXiv:2107.08785*, 2021.

Hadi Fanaee-T and Joao Gama. Event Labeling Combining Ensemble Detectors and Background Knowledge. *Progress in Artificial Intelligence*, 2(2):113–127, 2014.

Yassir Fathullah and Mark J. F. Gales. Self-distribution distillation: efficient uncertainty estimation. In James Cussens and Kun Zhang (eds.), *Uncertainty in Artificial Intelligence, Proceedings of the Thirty-Eighth Conference on Uncertainty in Artificial Intelligence, UAI 2022, 1-5 August 2022, Eindhoven, The Netherlands*, volume 180 of *Proceedings of Machine Learning Research*, pp. 663–673. PMLR, 2022.

Ronald A Fisher. The use of multiple measurements in taxonomic problems. *Annals of eugenics*, 7(2): 179–188, 1936.

Stanislav Fort, Huiyi Hu, and Balaji Lakshminarayanan. Deep Ensembles: A Loss Landscape Perspective. *arXiv preprint arXiv:1912.02757*, 2019.

Stanislav Fort, Jie Ren, and Balaji Lakshminarayanan. Exploring the limits of out-of-distribution detection. In *Advances in Neural Information Processing Systems 34: Annual Conference on Neural Information Processing Systems 2021, NeurIPS 2021, December 6-14, 2021, virtual*, pp. 7068–7081, 2021.

Tiago M Fragoso, Wesley Bertoli, and Francisco Louzada. Bayesian model averaging: A systematic review and conceptual classification. *International Statistical Review*, 86(1):1–28, 2018.

Yarin Gal and Zoubin Ghahramani. Dropout as a Bayesian Approximation: Representing Model Uncertainty in Deep Learning. In *International conference on Machine Learning*, pp. 1050–1059, 2016.

Timur Garipov, Pavel Izmailov, Dmitrii Podoprikhin, Dmitry P. Vetrov, and Andrew Gordon Wilson. Loss surfaces, mode connectivity, and fast ensembling of dnns. In *Advances in Neural Information Processing Systems 31: Annual Conference on Neural Information Processing Systems 2018, NeurIPS 2018, December 3-8, 2018, Montréal, Canada*, pp. 8803–8812, 2018.

Jakob Gawlikowski, Sudipan Saha, Anna M. Kruspe, and Xiao Xiang Zhu. An advanced dirichlet prior network for out-of-distribution detection in remote sensing. *IEEE Trans. Geosci. Remote. Sens.*, 60:1–19, 2022.

Andrew Gelman, John B Carlin, Hal S Stern, and Donald B Rubin. *Bayesian Data Analysis*. Chapman and Hall/CRC, 1995.

J Gerritsma, R Onnink, and A Versluis. Geometry, Resistance and Stability of the Delft Systematic Yacht Hull Series. *International shipbuilding progress*, 28(328):276–297, 1981.

Florin C. Ghesu, Bogdan Georgescu, Eli Gibson, Sebastian Gündel, Mannudeep K. Kalra, Ramandeep Singh, Subba R. Digumarthy, Sasa Grbic, and Dorin Comaniciu. Quantifying and Leveraging Classification Uncertainty for Chest Radiograph Assessment. In *Medical Image Computing and Computer Assisted Intervention - MICCAI 2019 - 22nd International Conference, Shenzhen, China, October 13-17, 2019, Proceedings, Part VI*, volume 11769 of *Lecture Notes in Computer Science*, pp. 676–684. Springer, 2019.

C Lee Giles, Kurt D Bollacker, and Steve Lawrence. CiteSeer: An Automatic Citation Indexing System. In *Proceedings of the third ACM conference on Digital libraries*, pp. 89–98, 1998.

Ian J. Goodfellow, Yaroslav Bulatov, Julian Ibarz, Sacha Arnoud, and Vinay D. Shet. Multi-Digit Number Recognition from Street View Imagery using Deep Convolutional Neural Networks. In *2nd International Conference on Learning Representations, ICLR 2014, Banff, AB, Canada, April 14-16, 2014, Conference Track Proceedings*, 2014.

Will Grathwohl, Kuan-Chieh Wang, Jörn-Henrik Jacobsen, David Duvenaud, Mohammad Norouzi, and Kevin Swersky. Your Classifier is Secretly an Energy-Based Model and You Should Treat It Like One. In *8th International Conference on Learning Representations, ICLR 2020, Addis Ababa, Ethiopia, April 26-30, 2020*.

Ang Nan Gu, Christina Luong, Mohammad H. Jafari, Nathan Van Woudenberg, Hany Girgis, Purang Abolmaesumi, and Teresa Tsang. Efficient Echocardiogram View Classification with Sampling-Free Uncertainty Estimation. In *Simplifying Medical Ultrasound - Second International Workshop, ASMUS 2021, Held in Conjunction with MICCAI 2021, Strasbourg, France, September 27, 2021, Proceedings*, volume 12967 of *Lecture Notes in Computer Science*, pp. 139–148. Springer, 2021.

Chuan Guo, Geoff Pleiss, Yu Sun, and Kilian Q. Weinberger. On Calibration of Modern Neural Networks. In *Proceedings of the 34th International Conference on Machine Learning, ICML 2017, Sydney, NSW, Australia, 6-11 August 2017*, volume 70 of *Proceedings of Machine Learning Research*, pp. 1321–1330. PMLR, 2017.

David Harrison Jr and Daniel L Rubinfeld. Hedonic Housing Prices and the Demand for Clean Air. *Journal of environmental economics and management*, 5(1):81–102, 1978.

Manuel Haussmann, Sebastian Gerwinn, and Melih Kandemir. Bayesian Evidential Deep Learning with PAC Regularization. *arXiv preprint arXiv:1906.00816*, 2019.

Jakob Drachmann Havtorn, Jes Frellsen, Søren Hauberg, and Lars Maaløe. Hierarchical VAEs Know What They Don't Know. In *Proceedings of the 38th International Conference on Machine Learning, ICML 2021, 18-24 July 2021, Virtual Event*, volume 139 of *Proceedings of Machine Learning Research*, pp. 4117–4128. PMLR, 2021.

Matthias Hein, Maksym Andriushchenko, and Julian Bitterwolf. Why ReLU Networks Yield High-Confidence Predictions Far Away From the Training Data and How to Mitigate the Problem. In *IEEE Conference on Computer Vision and Pattern Recognition, CVPR 2019, Long Beach, CA, USA, June 16-20, 2019*, pp. 41–50. Computer Vision Foundation / IEEE, 2019.

Patrick Hemmer, Niklas Kühl, and Jakob Schöffer. Deal: Deep Evidential Active Learning for Image Classification. In *Deep Learning Applications, Volume 3*, pp. 171–192. Springer, 2022.

Charles T Hemphill, John J Godfrey, and George R Doddington. The ATIS Spoken Language Systems Pilot Corpus. In *Speech and Natural Language: Proceedings of a Workshop Held at Hidden Valley, Pennsylvania, June 24-27, 1990*, 1990.

Dan Hendrycks and Kevin Gimpel. A Baseline for Detecting Misclassified and Out-of-Distribution Examples in Neural Networks. In *5th International Conference on Learning Representations, ICLR 2017, Toulon, France, April 24-26, 2017, Conference Track Proceedings*, 2017.

José Miguel Hernández-Lobato and Ryan Adams. Probabilistic Backpropagation for Scalable Learning of Bayesian Neural Networks. In *International conference on machine learning*, pp. 1861–1869. PMLR, 2015.

Geoffrey Hinton, Oriol Vinyals, Jeff Dean, et al. Distilling the knowledge in a neural network. *arXiv preprint arXiv:1503.02531*, 2(7), 2015.

Geoffrey E Hinton and Drew Van Camp. Keeping the neural networks simple by minimizing the description length of the weights. In *Proceedings of the sixth annual conference on Computational learning theory*, pp. 5–13, 1993.

Weihua Hu, Matthias Fey, Marinka Zitnik, Yuxiao Dong, Hongyu Ren, Bowen Liu, Michele Catasta, and Jure Leskovec. Open Graph Benchmark: Datasets for Machine Learning on Graphs. *Advances in neural information processing systems*, 33:22118–22133, 2020.

Yibo Hu, Yuzhe Ou, Xujiang Zhao, Jin-Hee Cho, and Feng Chen. Multidimensional Uncertainty-Aware Evidential Neural Networks. In *Thirty-Fifth AAAI Conference on Artificial Intelligence, AAAI 2021, Thirty-Third Conference on Innovative Applications of Artificial Intelligence, IAAI 2021, The Eleventh Symposium on Educational Advances in Artificial Intelligence, EAAI 2021, Virtual Event, February 2-9, 2021*, pp. 7815–7822. AAAI Press, 2021.

Xinyu Huang, Xinjing Cheng, Qichuan Geng, Binbin Cao, Dingfu Zhou, Peng Wang, Yuanqing Lin, and Ruigang Yang. The Apolloscape Dataset for Autonomous Driving. In *Proceedings of the IEEE conference on computer vision and pattern recognition workshops*, pp. 954–960, 2018.

Eyke Hüllermeier. Quantifying aleatoric and epistemic uncertainty in machine learning: Are conditional entropy and mutual information appropriate measures? *arXiv preprint arXiv:2209.03302*, 2022.

Eyke Hüllermeier and Willem Waegeman. Aleatoric and Epistemic Uncertainty in Machine Learning: An Introduction to Concepts and Methods. *Mach. Learn.*, 110(3):457–506, 2021.

Andrew Ilyas, Shibani Santurkar, Dimitris Tsipras, Logan Engstrom, Brandon Tran, and Aleksander Madry. Adversarial Examples Are Not Bugs, They Are Features. In *Advances in Neural Information Processing Systems 32: Annual Conference on Neural Information Processing Systems 2019, NeurIPS 2019, December 8-14, 2019, Vancouver, BC, Canada*, pp. 125–136, 2019.

Pavel Izmailov, Patrick Nicholson, Sanae Lotfi, and Andrew G Wilson. Dangers of bayesian model averaging under covariate shift. *Advances in Neural Information Processing Systems*, 34:3309–3322, 2021a.

Pavel Izmailov, Sharad Vikram, Matthew D. Hoffman, and Andrew Gordon Wilson. What Are Bayesian Neural Network Posteriors Really Like? In *Proceedings of the 38th International Conference on Machine Learning, ICML 2021, 18-24 July 2021, Virtual Event*, volume 139 of *Proceedings of Machine Learning Research*, pp. 4629–4640. PMLR, 2021b.

Alon Jacovi, Ana Marasović, Tim Miller, and Yoav Goldberg. Formalizing trust in artificial intelligence: Prerequisites, causes and goals of human trust in ai. In *Proceedings of the 2021 ACM conference on fairness, accountability, and transparency*, pp. 624–635, 2021.

Moksh Jain, Salem Lahlou, Hadi Nekoei, Victor Butoi, Paul Bertin, Jarrid Rector-Brooks, Maksym Korablyov, and Yoshua Bengio. Deup: Direct epistemic uncertainty prediction. *arXiv preprint arXiv:2102.08501*, 2021.

Harold Jeffreys. *The Theory of Probability*. OUP Oxford, 1998.

Robin Jia, Larry Heck, Dilek Hakkani-Tür, and Georgi Nikolov. Learning Concepts through Conversations in Spoken Dialogue Systems. In *2017 IEEE International Conference on Acoustics, Speech and Signal Processing (ICASSP)*, pp. 5725–5729. IEEE, 2017.

Taejong Joo, Uijung Chung, and Min-Gwan Seo. Being Bayesian about Categorical Probability. *CoRR*, abs/2002.07965, 2020.

Michael I Jordan, Zoubin Ghahramani, Tommi S Jaakkola, and Lawrence K Saul. An Introduction to Variational Methods for Graphical Models. *Machine learning*, 37(2):183–233, 1999.

Jeevesh Juneja, Rachit Bansal, Kyunghyun Cho, João Sedoc, and Naomi Saphra. Linear connectivity reveals generalization strategies. *arXiv preprint arXiv:2205.12411*, 2022.

Alex Kendall and Yarin Gal. What uncertainties do we need in bayesian deep learning for computer vision? *Advances in neural information processing systems*, 30, 2017.

Sunghwan Kim, Jie Chen, Tiejun Cheng, Asta Gindulyte, Jia He, Siqian He, Qingliang Li, Benjamin A Shoemaker, Paul A Thiessen, Bo Yu, et al. PubChem 2019 Update: Improved Access to Chemical Data. *Nucleic acids research*, 47(D1):D1102–D1109, 2019.

Diederik P. Kingma and Jimmy Ba. Adam: A method for stochastic optimization. In Yoshua Bengio and Yann LeCun (eds.), *3rd International Conference on Learning Representations, ICLR 2015, San Diego, CA, USA, May 7-9, 2015, Conference Track Proceedings*, 2015.

Diederik P. Kingma and Max Welling. Auto-Encoding Variational Bayes. In *2nd International Conference on Learning Representations, ICLR 2014, Banff, AB, Canada, April 14-16, 2014, Conference Track Proceedings*, 2014.

Johannes Klicpera, Aleksandar Bojchevski, and Stephan Günnemann. Predict then propagate: Graph neural networks meet personalized pagerank. In *7th International Conference on Learning Representations, ICLR 2019, New Orleans, LA, USA, May 6-9, 2019*, 2019.

Benjamin Kompa, Jasper Snoek, and Andrew L. Beam. Empirical frequentist coverage of deep learning uncertainty quantification procedures. *Entropy*, 23(12):1608, 2021.

Anna-Kathrin Kopetzki, Bertrand Charpentier, Daniel Zügner, Sandhya Giri, and Stephan Günnemann. Evaluating Robustness of Predictive Uncertainty Estimation: Are Dirichlet-based Models Reliable? In *Proceedings of the 38th International Conference on Machine Learning, ICML 2021, 18-24 July 2021, Virtual Event*, volume 139 of *Proceedings of Machine Learning Research*, pp. 5707–5718. PMLR, 2021.

Agustinus Kristiadi, Matthias Hein, and Philipp Hennig. Being Bayesian, Even Just a Bit, Fixes Overconfidence in ReLU Networks. In *Proceedings of the 37th International Conference on Machine Learning, ICML 2020, 13-18 July 2020, Virtual Event*, volume 119 of *Proceedings of Machine Learning Research*, pp. 5436–5446. PMLR, 2020.

Alex Krizhevsky, Geoffrey Hinton, et al. Learning Multiple Layers of Features from Tiny Images. 2009.

Meelis Kull, Miquel Perello Nieto, Markus Kängsepp, Telmo Silva Filho, Hao Song, and Peter Flach. Beyond Temperature Scaling: Obtaining Well-Calibrated Multi-Class Probabilities with Dirichlet Calibration. *Advances in neural information processing systems*, 32, 2019.

Morton Kupperman. Probabilities of Hypotheses and Information-Statistics in Sampling from Exponential-Class Populations. *Selected Mathematical Papers*, 29(2):57, 1964.

Alexey Kurakin, Ian J. Goodfellow, and Samy Bengio. Adversarial Examples in the Physical World. In *5th International Conference on Learning Representations, ICLR 2017, Toulon, France, April 24-26, 2017, Workshop Track Proceedings*, 2017.

Brenden M Lake, Ruslan Salakhutdinov, and Joshua B Tenenbaum. Human-Level Concept Learning Through Probabilistic Program Induction. *Science*, 350(6266):1332–1338, 2015.

Balaji Lakshminarayanan, Alexander Pritzel, and Charles Blundell. Simple and Scalable Predictive Uncertainty Estimation using Deep Ensembles. In *Advances in neural information processing systems*, pp. 6402–6413, 2017.

Yann LeCun. The MNIST Database of Handwritten Digits, 1998. URL http://yann.lecun.com/exdb/mnist/.

Yann LeCun, Léon Bottou, Yoshua Bengio, and Patrick Haffner. Gradient-Based Learning Applied to Document Recognition. *Proceedings of the IEEE*, 86(11):2278–2324, 1998.

Kimin Lee, Kibok Lee, Honglak Lee, and Jinwoo Shin. A Simple Unified Framework for Detecting Out-of-Distribution Samples and Adversarial Attacks. In *Advances in Neural Information Processing Systems 31: Annual Conference on Neural Information Processing Systems 2018, NeurIPS 2018, December 3-8, 2018, Montréal, Canada*, pp. 7167–7177, 2018.

Jing Lei and Larry Wasserman. Distribution-free prediction bands for non-parametric regression. *Journal of the Royal Statistical Society: Series B (Statistical Methodology)*, 76(1):71–96, 2014.

Hao Li, Yang Nan, Javier Del Ser, and Guang Yang. Region-based evidential deep learning to quantify uncertainty and improve robustness of brain tumor segmentation. *arXiv preprint arXiv:2208.06038*, 2022.

Shiyu Liang, Yixuan Li, and R. Srikant. Enhancing The Reliability of Out-of-distribution Image Detection in Neural Networks. In *6th International Conference on Learning Representations, ICLR 2018, Vancouver, BC, Canada, April 30 - May 3, 2018, Conference Track Proceedings*, 2018.

Q. Vera Liao and S. Shyam Sundar. Designing for responsible trust in AI systems: A communication perspective. In *FAccT '22: 2022 ACM Conference on Fairness, Accountability, and Transparency, Seoul, Republic of Korea, June 21 - 24, 2022*, pp. 1257–1268. ACM, 2022.

Jiayu Lin. On the Dirichlet Distribution. *Mater's Report*, 2016.

Jeremiah Z. Liu, Zi Lin, Shreyas Padhy, Dustin Tran, Tania Bedrax-Weiss, and Balaji Lakshminarayanan. Simple and Principled Uncertainty Estimation with Deterministic Deep Learning via Distance Awareness. In *Advances in Neural Information Processing Systems 33: Annual Conference on Neural Information Processing Systems 2020, NeurIPS 2020, December 6-12, 2020, virtual*, 2020.

Tiqing Liu, Yuhmei Lin, Xin Wen, Robert N Jorissen, and Michael K Gilson. BindingDB: A Web-Accessible Database of Experimentally Determined Protein–Ligand Binding Affinities. *Nucleic acids research*, 35 (suppl_1):D198–D201, 2007.

Zhijian Liu, Alexander Amini, Sibo Zhu, Sertac Karaman, Song Han, and Daniela L. Rus. Efficient and Robust LiDAR-Based End-to-End Navigation. In *IEEE International Conference on Robotics and Automation, ICRA 2021, Xi'an, China, May 30 - June 5, 2021*, pp. 13247–13254. IEEE, 2021.

Ziwei Liu, Ping Luo, Xiaogang Wang, and Xiaoou Tang. Deep Learning Face Attributes in the Wild. In *Proceedings of the IEEE international conference on computer vision*, pp. 3730–3738, 2015.

David JC MacKay. Developments in probabilistic modelling with neural networks—ensemble learning. In *Neural Networks: Artificial Intelligence and Industrial Applications*, pp. 191–198. Springer, 1995.

David John Cameron Mackay. *Bayesian methods for adaptive models*. California Institute of Technology, 1992.

Andrey Malinin and Mark J. F. Gales. Predictive Uncertainty Estimation via Prior Networks. In *Advances in Neural Information Processing Systems 31: Annual Conference on Neural Information Processing Systems 2018, NeurIPS 2018, 3-8 December 2018, Montréal, Canada*, pp. 7047–7058, 2018.

Andrey Malinin and Mark J. F. Gales. Reverse KL-Divergence Training of Prior Networks: Improved Uncertainty and Adversarial Robustness. In *Advances in Neural Information Processing Systems 32: Annual Conference on Neural Information Processing Systems 2019, NeurIPS 2019, 8-14 December 2019, Vancouver, BC, Canada*, pp. 14520–14531, 2019.

Andrey Malinin, Sergey Chervontsev, Ivan Provilkov, and Mark Gales. Regression Prior Networks. *arXiv preprint arXiv:2006.11590*, 2020a.

Andrey Malinin, Bruno Mlodozeniec, and Mark J. F. Gales. Ensemble Distribution Distillation. In *8th International Conference on Learning Representations, ICLR 2020, Addis Ababa, Ethiopia, April 26-30, 2020*, 2020b.

Lei Mao. Introduction to Exponential Family, 2019. URL `https://zhiyzuo.github.io/Exponential-Family-Distributions/`. Accessed April 2022.

Andrés R. Masegosa. Learning under Model Misspecification: Applications to Variational and Ensemble methods. In *Advances in Neural Information Processing Systems 33: Annual Conference on Neural Information Processing Systems 2020, NeurIPS 2020, December 6-12, 2020, virtual*, 2020.

Julian McAuley, Christopher Targett, Qinfeng Shi, and Anton Van Den Hengel. Image-Based Recommendations on Styles and Substitutes. In *Proceedings of the 38th international ACM SIGIR conference on research and development in information retrieval*, pp. 43–52, 2015.

Andrew Kachites McCallum, Kamal Nigam, Jason Rennie, and Kristie Seymore. Automating the Construction of Internet Portals with Machine Learning. *Information Retrieval*, 3(2):127–163, 2000.

Nis Meinert and Alexander Lavin. Multivariate Deep Evidential Regression. *arXiv preprint arXiv:2104.06135*, 2021.

Moritz Menze and Andreas Geiger. Object Scene Flow for Autonomous Vehicles. In *Proceedings of the IEEE conference on computer vision and pattern recognition*, pp. 3061–3070, 2015.

Jeffrey W. Miller. (ML 7.7.A2) Expectation of a Dirichlet Random Variable, 2011. URL `https://www.youtube.com/watch?v=emnfq4txDuI`.

Matthias Minderer, Josip Djolonga, Rob Romijnders, Frances Hubis, Xiaohua Zhai, Neil Houlsby, Dustin Tran, and Mario Lucic. Revisiting the calibration of modern neural networks. *Advances in Neural Information Processing Systems*, 34:15682–15694, 2021.

Jose G Moreno-Torres, Troy Raeder, RocíO Alaiz-RodríGuez, Nitesh V Chawla, and Francisco Herrera. A Unifying View on Dataset Shift in Classification. *Pattern recognition*, 45(1):521–530, 2012.

Jishnu Mukhoti, Andreas Kirsch, Joost van Amersfoort, Philip HS Torr, and Yarin Gal. Deterministic Neural Networks With Appropriate Inductive Biases Capture Epistemic and Aleatoric Uncertainty. *arXiv preprint arXiv:2102.11582*, 2021.

Kevin P Murphy. Conjugate Bayesian Analysis of the Gaussian Distribution. 2007.

Vaishnavh Nagarajan, Anders Andreassen, and Behnam Neyshabur. Understanding the Failure Modes of Out-Of-Distribution Generalization. In *9th International Conference on Learning Representations, ICLR 2021, Virtual Event, Austria, May 3-7, 2021*, 2021.

Eric T. Nalisnick, Akihiro Matsukawa, Yee Whye Teh, Dilan Görür, and Balaji Lakshminarayanan. Do Deep Generative Models Know What They Don't Know? In *7th International Conference on Learning Representations, ICLR 2019, New Orleans, LA, USA, May 6-9, 2019*, 2019.

Galileo Namata, Ben London, Lise Getoor, Bert Huang, and UMD EDU. Query-Driven Active Surveying for Collective Classification. In *10th International Workshop on Mining and Learning with Graphs*, volume 8, pp. 1, 2012.

Jay Nandy, Wynne Hsu, and Mong Li Lee. Towards Maximizing the Representation Gap between In-Domain & Out-of-Distribution Examples. *Advances in Neural Information Processing Systems*, 33, 2020.

Radford M Neal. *Bayesian learning for neural networks*, volume 118. Springer Science & Business Media, 2012.

Jeremy Nixon, Michael W Dusenberry, Linchuan Zhang, Ghassen Jerfel, and Dustin Tran. Measuring calibration in deep learning. In *CVPR Workshops*, volume 2, 2019.

Dongpin Oh and Bonggun Shin. Improving evidential deep learning via multi-task learning. In *Proceedings of the AAAI Conference on Artificial Intelligence*, volume 36, pp. 7895–7903, 2022.

Yaniv Ovadia, Emily Fertig, Jie Ren, Zachary Nado, David Sculley, Sebastian Nowozin, Joshua Dillon, Balaji Lakshminarayanan, and Jasper Snoek. Can You Trust Your Model's Uncertainty? Evaluating Predictive Uncertainty under Dataset Shift. In *Advances in Neural Information Processing Systems*, pp. 13991–14002, 2019.

Harris Papadopoulos, Kostas Proedrou, Volodya Vovk, and Alex Gammerman. Inductive confidence machines for regression. In *European Conference on Machine Learning*, pp. 345–356. Springer, 2002.

Fabian Paschke, Christian Bayer, Martyna Bator, Uwe Mönks, Alexander Dicks, Olaf Enge-Rosenblatt, and Volker Lohweg. Sensorlose Zustandsüberwachung an Synchronmotoren. In *Proc*, pp. 211, 2013.

Tim Pearce, Alexandra Brintrup, and Jun Zhu. Understanding Softmax Confidence and Uncertainty. *arXiv preprint arXiv:2106.04972*, 2021.

F. Pedregosa, G. Varoquaux, A. Gramfort, V. Michel, B. Thirion, O. Grisel, M. Blondel, P. Prettenhofer, R. Weiss, V. Dubourg, J. Vanderplas, A. Passos, D. Cournapeau, M. Brucher, M. Perrot, and E. Duchesnay. Scikit-learn: Machine learning in Python. *Journal of Machine Learning Research*, 12:2825–2830, 2011.

Kürsat Petek, Kshitij Sirohi, Daniel Büscher, and Wolfram Burgard. Robust monocular localization in sparse HD maps leveraging multi-task uncertainty estimation. In *2022 International Conference on Robotics and Automation, ICRA 2022, Philadelphia, PA, USA, May 23-27, 2022*, pp. 4163–4169. IEEE, 2022.

Stefan T Radev, Marco D'Alessandro, Ulf K Mertens, Andreas Voss, Ullrich Köthe, and Paul-Christian Bürkner. Amortized Bayesian Model Comparison with Evidential Deep Learning. *IEEE Transactions on Neural Networks and Learning Systems*, 2021.

Danilo Jimenez Rezende and Shakir Mohamed. Variational Inference with Normalizing Flows. In *Proceedings of the 32nd International Conference on Machine Learning, ICML 2015, Lille, France, 6-11 July 2015*, volume 37 of *JMLR Workshop and Conference Proceedings*, pp. 1530–1538. JMLR.org, 2015.

Murat Sensoy, Lance Kaplan, and Melih Kandemir. Evidential Deep Learning to Quantify Classification Uncertainty. In *Advances in Neural Information Processing Systems*, pp. 3179–3189, 2018.

Murat Sensoy, Lance M. Kaplan, Federico Cerutti, and Maryam Saleki. Uncertainty-Aware Deep Classifiers Using Generative Models. In *The Thirty-Fourth AAAI Conference on Artificial Intelligence, AAAI 2020, The Thirty-Second Innovative Applications of Artificial Intelligence Conference, IAAI 2020, The Tenth AAAI Symposium on Educational Advances in Artificial Intelligence, EAAI 2020, New York, NY, USA, February 7-12, 2020*, pp. 5620–5627. AAAI Press, 2020.

Oleksandr Shchur, Maximilian Mumme, Aleksandar Bojchevski, and Stephan Günnemann. Pitfalls of Graph Neural Network Evaluation. *arXiv preprint arXiv:1811.05868*, 2018.

Maohao Shen, Yuheng Bu, Prasanna Sattigeri, Soumya Ghosh, Subhro Das, and Gregory Wornell. Post-hoc uncertainty learning using a dirichlet meta-model. *arXiv preprint arXiv:2212.07359*, 2022.

Yilin Shen, Wenhu Chen, and Hongxia Jin. Modeling Token-level Uncertainty to Learn Unknown Concepts in SLU via Calibrated Dirichlet Prior RNN. *CoRR*, abs/2010.08101, 2020.

Nathan Silberman, Derek Hoiem, Pushmeet Kohli, and Rob Fergus. Indoor Segmentation and Support Inference from RGBD Images. In *European conference on computer vision*, pp. 746–760. Springer, 2012.

Lewis Smith and Yarin Gal. Understanding Measures of Uncertainty for Adversarial Example Detection. In *Proceedings of the Thirty-Fourth Conference on Uncertainty in Artificial Intelligence, UAI 2018, Monterey, California, USA, August 6-10, 2018*, pp. 560–569, 2018.

Ava P Soleimany, Alexander Amini, Samuel Goldman, Daniela Rus, Sangeeta N Bhatia, and Connor W Coley. Evidential Deep Learning for Guided Molecular Property Prediction and Discovery. *ACS central science*, 7(8):1356–1367, 2021.

Maximilian Stadler, Bertrand Charpentier, Simon Geisler, Daniel Zügner, and Stephan Günnemann. Graph Posterior Network: Bayesian Predictive Uncertainty for Node Classification. *Advances in Neural Information Processing Systems*, 34, 2021.

Jing Tang, Agnieszka Szwajda, Sushil Shakyawar, Tao Xu, Petteri Hintsanen, Krister Wennerberg, and Tero Aittokallio. Making Sense of Large-Scale Kinase Inhibitor Bioactivity Data Sets: A Comparative and Integrative Analysis. *Journal of Chemical Information and Modeling*, 54(3):735–743, 2014.

Athanasios Tsanas and Angeliki Xifara. Accurate Quantitative Estimation of Energy Performance of Residential Buildings using Statistical Machine Learning Tools. *Energy and buildings*, 49:560–567, 2012.

Theodoros Tsiligkaridis. Information Robust Dirichlet Networks for Predictive Uncertainty Estimation. *arXiv preprint arXiv:1910.04819*, 2019.

Dennis Ulmer and Giovanni Cinà. Know Your Limits: Uncertainty Estimation with ReLU Classifiers Fails at Reliable OOD Detection. In *Uncertainty in Artificial Intelligence*, pp. 1766–1776. PMLR, 2021.

Dennis Ulmer, Lotta Meijerink, and Giovanni Cinà. Trust Issues: Uncertainty Estimation Does not Enable Reliable OOD Detection on Medical Tabular Data. In *Machine Learning for Health*, pp. 341–354. PMLR, 2020.

Dennis Ulmer, Jes Frellsen, and Christian Hardmeier. Exploring predictive uncertainty and calibration in nlp: A study on the impact of method & data scarcity. *arXiv preprint arXiv:2210.15452*, 2022.

Joost van Amersfoort, Lewis Smith, Yee Whye Teh, and Yarin Gal. Uncertainty Estimation Using a Single Deep Deterministic Neural Network. In *Proceedings of the 37th International Conference on Machine Learning, ICML 2020, 13-18 July 2020, Virtual Event*, volume 119 of *Proceedings of Machine Learning Research*, pp. 9690–9700. PMLR, 2020.

Joost van Amersfoort, Lewis Smith, Andrew Jesson, Oscar Key, and Yarin Gal. On Feature Collapse and Deep Kernel Learning for Single Forward Pass Uncertainty. *arXiv preprint arXiv:2102.11409*, 2021.

Tim van Erven and Peter Harremoës. Rényi Divergence and Kullback-Leibler Divergence. *IEEE Trans. Inf. Theory*, 60(7):3797–3820, 2014.

Jordy Van Landeghem, Matthew Blaschko, Bertrand Anckaert, and Marie-Francine Moens. Benchmarking Scalable Predictive Uncertainty in Text Classification. *Ieee Access*, 10:43703–43737, 2022.

Vladimir Vovk, Alexander Gammerman, and Glenn Shafer. *Algorithmic learning in a random world*. Springer Science & Business Media, 2005.

Chen Wang, Xiang Wang, Jiawei Zhang, Liang Zhang, Xiao Bai, Xin Ning, Jun Zhou, and Edwin Hancock. Uncertainty Estimation for Stereo Matching Based on Evidential Deep Learning. *Pattern Recognition*, pp. 108498, 2021a.

Deng-Bao Wang, Lei Feng, and Min-Ling Zhang. Rethinking calibration of deep neural networks: Do not be afraid of overconfidence. *Advances in Neural Information Processing Systems*, 34:11809–11820, 2021b.

Xiang Wei, Boqing Gong, Zixia Liu, Wei Lu, and Liqiang Wang. Improving the Improved Training of Wasserstein GANs: A Consistency Term and Its Dual Effect. In *6th International Conference on Learning Representations, ICLR 2018, Vancouver, BC, Canada, April 30 - May 3, 2018, Conference Track Proceedings*, 2018.

Florian Wenzel, Kevin Roth, Bastiaan S Veeling, Jakub Świątkowski, Linh Tran, Stephan Mandt, Jasper Snoek, Tim Salimans, Rodolphe Jenatton, and Sebastian Nowozin. How Good is the Bayes Posterior in Deep Neural Networks Really? *arXiv preprint arXiv:2002.02405*, 2020.

Wikimedia Commons. Iris setosa, 2022a. URL https://en.wikipedia.org/wiki/Iris_setosa. File:Irissetosa1.jpg.

Wikimedia Commons. Iris versicolor, 2022b. URL https://en.wikipedia.org/wiki/Iris_versicolor. File:Blue_Flag,_Ottawa.jpg.

Wikimedia Commons. Iris virginica, 2022c. URL https://en.wikipedia.org/wiki/Iris_virginica#/media/File:Iris_virginica_2.jpg. File:Iris_virginica_2.jpg.

Andrew Gordon Wilson and Pavel Izmailov. Bayesian Deep Learning and a Probabilistic Perspective of Generalization. In *Advances in Neural Information Processing Systems 33: Annual Conference on Neural Information Processing Systems 2020, NeurIPS 2020, December 6-12, 2020, virtual*, 2020.

John Michael Winn. Variational Message Passing and Its Applications. 2004.

Jae Oh Woo. Analytic mutual information in bayesian neural networks. In *IEEE International Symposium on Information Theory, ISIT 2022, Espoo, Finland, June 26 - July 1, 2022*, pp. 300–305. IEEE, 2022.

Han Xiao, Kashif Rasul, and Roland Vollgraf. Fashion-MNIST: A Novel Image Dataset for Benchmarking Machine Learning Algorithms. *arXiv preprint arXiv:1708.07747*, 2017.

Jianxiong Xiao, James Hays, Krista A Ehinger, Aude Oliva, and Antonio Torralba. Sun Database: Large-scale Scene Recognition from Abbey to Zoo. In *2010 IEEE computer society conference on computer vision and pattern recognition*, pp. 3485–3492. IEEE, 2010.

Ronald R Yager and Liping Liu. *Classic Works of the Dempster-Shafer Theory of Belief Functions*, volume 219. Springer, 2008.

I-C Yeh. Modeling of Strength of High-Performance Concrete using Artificial Neural Networks. *Cement and Concrete research*, 28(12):1797–1808, 1998.

Fisher Yu, Ari Seff, Yinda Zhang, Shuran Song, Thomas Funkhouser, and Jianxiong Xiao. LSUN: Construction of a Large-Scale Image Dataset using Deep Learning with Humans in the Loop. *arXiv preprint arXiv:1506.03365*, 2015.

Fuxun Yu, Zhuwei Qin, Chenchen Liu, Liang Zhao, Yanzhi Wang, and Xiang Chen. Interpreting and Evaluating Neural Network Robustness. In *Proceedings of the Twenty-Eighth International Joint Conference on Artificial Intelligence, IJCAI 2019, Macao, China, August 10-16, 2019*, pp. 4199–4205. ijcai.org, 2019.

Chrysoula Zerva, Taisiya Glushkova, Ricardo Rei, and André FT Martins. Better uncertainty quantification for machine translation evaluation. *arXiv preprint arXiv:2204.06546*, 2022.

Xujiang Zhao, Yuzhe Ou, Lance Kaplan, Feng Chen, and Jin-Hee Cho. Quantifying Classification Uncertainty Using Regularized Evidential Neural Networks. *arXiv preprint arXiv:1910.06864*, 2019.

Xujiang Zhao, Feng Chen, Shu Hu, and Jin-Hee Cho. Uncertainty Aware Semi-Supervised Learning on Graph Data. In *Advances in Neural Information Processing Systems 33: Annual Conference on Neural Information Processing Systems 2020, NeurIPS 2020, December 6-12, 2020, virtual*, 2020.

A Code Appendix

A.1 Iris Example Training Details

The code used to produce Figure 2 is available online.[14] All models use three layers with 100 hidden units and ReLU activations each. We furthermore optimized all of the models with a learning rate of 0.001 using the Adam optimizer (Kingma & Ba, 2015) with its default parameter settings. We also regularize the ensemble and MC Dropout model with a dropout probability of 0.1 each.

Prior Network specifics We choose the expected l_2 loss by Sensoy et al. (2018) and regularize the network using the KL divergence w.r.t. to a uniform Dirichlet as in Sensoy et al. (2018). In the regularization term, we do not use the original concentration parameters $\boldsymbol{\alpha}$, but a version in which the concentration of the parameter α_k corresponding to the correct class is removed using a one-hot label encoding $\mathbf{y}$ by $\tilde{\boldsymbol{\alpha}} = (1-\boldsymbol{\alpha}) \odot \boldsymbol{\alpha} + \mathbf{y} \odot \boldsymbol{\alpha}$, where $\odot$ denotes point-wise multiplication. The regularization term is added to the loss using a weighting factor of 0.05.

A.2 Code Availability

We list the available code repositories for surveyed works in Table 4. Works for which no official implementation could be found are not listed.

B Datasets & Evaluation Techniques Appendix

This section contains a discussion of the used datasets, methods to evaluate the quality of uncertainty evaluation, as well as a direct of available models based on the reported results to determine the most useful choices for practitioners. An overview over the differences between the surveyed works is given in Table 5.

Datasets Most models are applied to image classification problems, where popular choices involve the MNIST dataset (LeCun, 1998), using as OOD datasets Fashion-MNIST (Xiao et al., 2017), notMNIST (Bulatov, 2011) containing English letters, K-MNIST (Clanuwat et al., 2018) with ancient Japanese Kuzushiji characters, and the Omniglot dataset (Lake et al., 2015), featuring handwritten characters from more than 50 alphabets. Other choices involve different versions of the CIFAR-10 object recognition dataset (LeCun et al., 1998; Krizhevsky et al., 2009) for training purposes and SVHN (Goodfellow et al., 2014), iSUN (Xiao et al., 2010), LSUN (Yu et al., 2015), CelebA (Liu et al., 2015), ImageNet (Deng et al., 2009) and TinyImagenet (Bastidas, 2017) for OOD samples. Regression image datasets include for instance the NYU Depth Estimation v2 dataset (Silberman et al., 2012), using ApolloScape (Huang et al., 2018) or KITTI (Menze & Geiger, 2015) as an OOD dataset. Many authors also illustrate model uncertainty on synthetic data, for instance by simulating clusters of data points using Gaussians (Malinin & Gales, 2018; 2019; Nandy et al., 2020; Zhao et al., 2019; Hu et al., 2020; Charpentier et al., 2020; 2022), spiral data (Malinin et al., 2020b) or polynomials for regression (Amini et al., 2020; Oh & Shin, 2022; Meinert & Lavin, 2021; Malinin et al., 2020a; Charpentier et al., 2022). Tabular datasets include the Segment dataset, predicting image segments based on pixel features (Dua et al., 2017), and the sensorless drive dataset (Dua et al., 2017; Paschke et al., 2013), describing the maintenance state of electric current drives as well as popular regression datasets included in the UCI regression benchmark used by Hernández-Lobato & Adams (2015); Gal & Ghahramani (2016): Boston house prices (Harrison Jr & Rubinfeld, 1978), concrete compression strength (Yeh, 1998), energy efficiency of buildings (Tsanas & Xifara, 2012), forward kinematics of an eight link robot arm (Corke, 1996), maintenance of naval propulsion systems (Coraddu et al., 2016), properties of protein tertiary stuctures, wine quality (Cortez et al., 2009), and yacht hydrodynamics (Gerritsma et al., 1981). Furthermore, Oh & Shin (2022) use a number of drug discovery datasets, such as Davis (Davis et al., 2011), Kiba (Tang et al., 2014), BindingDB (Liu et al., 2007) and PubChem (Kim et al., 2019). Biloš et al. (2019) are the only authors working on asynchronous time even prediction, and supply their own data in the form of processed stack exchange postings, smart home data, and car indicators.

[14] Code will be made available upon acceptance.

Table 4: Overview over code repositories of surveyed works.

Paper	Code Repository
Prior network (Malinin & Gales, 2018)	https://github.com/KaosEngineer/PriorNetworks-OLD
Prior networks (Malinin & Gales, 2019)	https://github.com/KaosEngineer/PriorNetworks
Dirichlet via Function Decomposition (Biloš et al., 2019)	https://github.com/sharpenb/Uncertainty-Event-Prediction
Prior network with PAC Regularization (Haussmann et al., 2019)	https://github.com/manuelhaussmann/bedl
Prior networks with representation gap (Nandy et al., 2020)	https://github.com/jayjaynandy/maximize-representation-gap
Graph-based Kernel Dirichlet distribution estimation (GKDE) (Zhao et al., 2020)	https://github.com/zxj32/uncertainty-GNN
Evidential Deep Learning (Sensoy et al., 2018)	https://muratsensoy.github.io/uncertainty.html
WGAN–ENN (Hu et al., 2021)	https://github.com/snowood1/wenn
Belief Matching (Joo et al., 2020)	https://github.com/tjoo512/belief-matching-framework
Posterior Networks (Charpentier et al., 2020)	https://github.com/sharpenb/Posterior-Network
Graph Posterior Networks (Stadler et al., 2021)	https://github.com/stadlmax/Graph-Posterior-Network
Generative Evidential Neural Networks (Sensoy et al., 2020)	https://muratsensoy.github.io/gen.html
Deep Evidential Regression with Multi-task Learning (Oh & Shin, 2022)	https://github.com/deargen/MT-ENet
Multivariate Deep Evidential Regression (Meinert & Lavin, 2021)	https://github.com/avitase/mder/
Regression Prior Network (Malinin et al., 2020a)	https://github.com/JanRocketMan/regression-prior-networks
Natural Posterior Network (Charpentier et al., 2022)	https://github.com/borchero/natural-posterior-network

Shen et al. (2020) provide the sole method on language data, and use three different concept learning datasets, i.e. Concept Learning (Jia et al., 2017), Snips (Coucke et al., 2018) and ATIS (Hemphill et al., 1990), which contains new OOD concepts to be learned by design. For graph neural networks, Zhao et al. (2020) and Stadler et al. (2021) select data from the co-purchase datasets Amazon Computer, Amazon Photos (McAuley et al., 2015) and the CoraML (McCallum et al., 2000), CiteSeer (Giles et al., 1998) and PubMed (Namata et al., 2012), Coauthors Physics (Shchur et al., 2018), CoauthorCS (Namata et al., 2012) and OGBN Arxiv (Hu et al., 2020) citation datasets. Lastly, Charpentier et al. (2022) use a single count prediction dataset concerned with predicting the number of bike rentals (Fanaee-T & Gama, 2014).

Uncertainty Evaluation Methods There usually are no gold labels for uncertainty estimates, which is why the efficacy of proposed solutions has to be evaluated in a different way. One such way used by almost all the surveyed works is using uncertainty estimates in a proxy OOD detection task: Since the model is underspecified on unseen samples from another distribution, it should be more uncertain. By labelling

OOD samples as the positive and ID inputs as the negative class, we can measure the performance of uncertainty estimates using the area under the receiver-operator characteristic (AUROC) or the area under the precision-recall curve (AUPR). We can thereby characterize the usage of data from another dataset as a form of covariate shift, while using left-out classes for testing can be seen as a kind of concept shift (Moreno-Torres et al., 2012). Instead of using OOD data, another approach is to use adversarial examples (Malinin & Gales, 2019; Tsiligkaridis, 2019; Sensoy et al., 2018; Hu et al., 2021; Chen et al., 2018; Amini et al., 2020), checking if they can be identified through uncertainty. In the case of Shen et al. (2020), OOD detection or new concept extraction is the actual and not a proxy task, and thus can be evaluated using classical metrics such as the F_1 score. Another way is misclassification detection: In general, we would desire the model to be more uncertain about inputs it incurs a higher loss on, i.e., what it is more wrong about. For this purpose, some works (Malinin & Gales, 2018; Zhao et al., 2020; Charpentier et al., 2020) measure whether let missclassified inputs be the positive class in another binary proxy classification test, and again measure AUROC and AUPR. Alternatively, Malinin et al. (2020b); Stadler et al. (2021); Amini et al. (2020) show or measure the area under the prediction / rejection curve, graphing how task performance varies as predictions on increasingly uncertain inputs is suspended. Lastly, some authors look at a model's calibration (Guo et al., 2017): While this does not allow to judge the quality of uncertainty estimates themselves, quantities like the expected calibration error quantify to what extent the output distribution of a classifier corresponds to the true label distribution, and thus whether aleatoric uncertainty is accurately reflected.

What is state-of-the-art? As apparent from Table 5, evaluation methods and datasets can vary tremendously between different research works. This can make it hard to accurately compare different approaches in a fair manner. Nevertheless, we try to draw some conclusion about the state-of-art in this research direction to the best extent possible: For **image classification**, the posterior (Charpentier et al., 2020) and natural posterior network (Charpentier et al., 2022) provide the best results on the tested benchmarks, both in terms of task performance and uncertainty quality. When the training an extra normalizing flow creates too much computational overhead, prior networks (Malinin & Gales, 2018) with the PAC-based regularizer (Haussmann et al., 2019; see Table 6 for final form) or a simple entropy regularizer (Appendix C.2) can be used. In the case of **regression** problems, the natural posterior network (Stadler et al., 2021) performs better or on par with the evidential regression by Amini et al. (2020) or an ensemble Lakshminarayanan et al. (2017) or MC Dropout (Gal & Ghahramani, 2016). For **graph neural networks**, the graph posterior network (Stadler et al., 2021) and a ensemble provide similar performance, but with the former displaying better uncertainty results. Again, this model requires training a NF, so a simpler fallback is provided by evidential regression (Amini et al., 2020) with the improvement by Oh & Shin (2022). For **NLP** and **count prediction**, the works of Shen et al. (2020) and Charpentier et al. (2022) are the only available instances from this model family, respectively. In the latter case, ensembles and the evidential regression framework (Amini et al., 2020) produce a lower root mean-squared error, but worse uncertainty estimates on OOD.

Caveats Stadler et al. (2021) point out that much of the ability of posterior networks stems from the addition of a NF, which have been shown to also sometimes behave unreliably on OOD data (Nalisnick et al., 2019). Although the NFs in posterior networks operate on the latent and not the feature space, they are also restricted to operate on features that the underlying network has learned to recognize. Recent work by Dietterich & Guyer (2022) has hinted at the fact that networks might identify OOD by the absence of known features, and not by the presence of new ones, providing a case in which posterior networks are likely to fail. Such evidence on OOD data and adversarial examples has indeed been identified by a study by Kopetzki et al. (2021). Exposing the model to (artificial) OOD data during training as done in the case of Malinin & Gales (2018; 2019); Nandy et al. (2020); Zhao et al. (2019) might alleviate this issue, but will never guarantee full coverage of all potential OOD cases. Lastly, Bengs et al. (2022) also prove how some of the used loss function used for training evidential models do not fulfill desiderata for epistemic uncertainty, pointing to a more fundamental flaw.

Table 5: Overview over uncertainty evaluation techniques and datasets. $^{(*)}$ indicates that a dataset was used as an OOD dataset for evaluation purposes, while $^{(\diamond)}$ signifies that it was used as an in-distribution or out-of-distribution dataset. $^{(\dagger)}$ means that a dataset was modified to create ID and OOD splits (for instance by removing some classes for evaluation or corrupting samples with noise).

		Data Modality		
Method	Uncertainty Evaluation	Images	Tabular	Other
Prior network (Malinin & Gales, 2018)	OOD Detection, Misclassification Detection	MNIST, CIFAR-10, Omniglot$^{(*)}$, SVHN$^{(*)}$, LSUN$^{(*)}$, TIM$^{(*)}$	✗	Clusters (Synthetic)
Prior networks (Malinin & Gales, 2019)	OOD Detection, Adversarial Attack Detection	MNIST, CIFAR-10/100, SVHN$^{(*)}$, LSUN$^{(*)}$, TIM$^{(*)}$	✗	Clusters (Synthetic)
Information Robust Dirichlet Networks (Tsiligkaridis, 2019)	OOD Detection, Adversarial Attack Detection	MNIST, FashionMNIST$^{(*)}$ notMNIST$^{(*)}$, Omniglot$^{(*)}$ CIFAR-10, TIM$^{(*)}$, SVHN$^{(*)}$	✗	✗
Dirichlet via Function Decomposition (Biloš et al., 2019)	OOD Detection	✗	Erdős-Rényi Graph (Synthetic), Stack Exchange, Smart Home, Car Indicators	✗
Prior network with PAC Regularization (Haussmann et al., 2019)	OOD Detection	MNIST, FashionMNIST$^{(*)}$ CIFAR-10$^{(\dagger)}$	✗	✗
Ensemble Distribution Distillation (Malinin et al., 2020b)	OOD Detection, Misclassification Detection, Calibration	CIFAR-10, CIFAR-100$^{(\diamond)}$ TIM$^{(\diamond)}$, LSUN$^{(*)}$	✗	Spirals (Synthetic)
Self-Distribution Distillation (Fathullah & Gales, 2022)	OOD Detection, Calibration	CIFAR-100 SVHN$^{(*)}$, LSUN$^{(*)}$	✗	✗
Prior networks with representation gap (Nandy et al., 2020)	OOD Detection	CIFAR-10$^{(\diamond)}$, CIFAR-100$^{(\diamond)}$ TIM, ImageNet$^{(*)}$	✗	Clusters (Synthetic)
Prior RNN (Shen et al., 2020)	New Concept Extraction	✗	✗	Concept Learning$^{(\diamond)}$, Snips$^{(\diamond)}$, ATIS$^{(\diamond)}$ (Language)
Graph-based Kernel Dirichlet distribution estimation (GKDE) (Zhao et al., 2020)	OOD Detection Misclassification Detection	✗	✗	Coauthors Physics$^{(\diamond)}$, Amazon Computer$^{(\diamond)}$ Amazon Photo$^{(\diamond)}$ (Graph)
Evidential Deep Learning (Sensoy et al., 2018)	OOD Detection, Adversarial Attack Detection	MNIST, notMNIST$^{(*)}$, CIFAR-10$^{(\dagger)}$	✗	✗
Regularized ENN Zhao et al. (2019)	OOD Detection	CIFAR-10$^{(\dagger)}$	✗	Clusters (Synthetic)
WGAN–ENN (Hu et al., 2021)	OOD Detection, Adversarial Attack Detection	MNIST, notMNIST$^{(*)}$, CIFAR-10$^{(\dagger)}$	✗	Clusters (Synthetic)
Variational Dirichlet (Chen et al., 2018)	OOD Detection, Adversarial Attack Detection	MNIST, CIFAR-10/100, iSUN$^{(*)}$, LSUN$^{(*)}$, SVHN$^{(*)}$, TIM$^{(*)}$	✗	✗
Dirichlet Meta-Model (Shen et al., 2022)	OOD Detection Misclassification Detection	MNIST$^{(\diamond,\dagger)}$, CIFAR-10$^{(\diamond,\dagger)}$, CIFAR-100$^{(\diamond)}$, Omniglot$^{(*)}$, FashionMNIST$^{(*)}$, K-MNIST$^{(*)}$, SVHN$^{(*)}$, LSUN$^{(*)}$, TIM$^{(*)}$	✗	✗
Belief Matching (Joo et al., 2020)	OOD Detection, Calibration	CIFAR-10/100, SVHN$^{(*)}$	✗	✗
Posterior Networks (Charpentier et al., 2020)	OOD Detection, Misclassification Detection, Calibration	MNIST, FashionMNIST$^{(*)}$, K-MNIST$^{(*)}$, CIFAR-10, SVHN$^{(*)}$	Segment$^{(\dagger)}$, Sensorless Drive$^{(\dagger)}$	Clusters (Synthetic)
Graph Posterior Networks (Stadler et al., 2021)	OOD Detection, Misclassification Detection, Calibration	✗	✗	Amazon Computer$^{(\diamond)}$, Amazon Photo$^{(\diamond)}$ CoraML$^{(\diamond)}$, CiteSeerCoraML$^{(\diamond)}$, PubMed$^{(\diamond)}$, Coauthors Physics$^{(\diamond)}$, CoauthorsCS$^{(\diamond)}$, OBGN Arxiv$^{(\diamond)}$ (Graph)
Deep Evidential Regression (Amini et al., 2020)	OOD Detection, Misclassification Detection, Adversarial Attack Detection Calibration	NYU Depth v2 ApolloScape* (Depth Estimation)	UCI Regression Benchmark	Univariate Regression (Synthetic)
Deep Evidential Regression with Multi-task Learning (Oh & Shin, 2022)	OOD Detection, Calibration	✗	Davis, Kiba$^{(\dagger)}$, BindingDB, PubChem$^{(*)}$ (Drug discovery), UCI Regression Benchmark	Univariate Regression (Synthetic)
Multivariate Deep Evidential Regression Meinert & Lavin (2021)	Qualitative Evaluation	✗	✗	Multivariate Regression (Synthetic)
Regression Prior Network (Malinin et al., 2020a)	OOD Detection	NYU Depth v2°, KITTI° (Depth Estimation)	UCI Regression Benchmark	Univariate Regression (Synthetic)
Natural Posterior Network (Charpentier et al., 2022)	OOD Detection, Calibration	NYU Depth v2, KITTI*, LSUN$^{(*)}$ (Depth Estimation), MNIST, FashionMNIST$^{(*)}$, K-MNIST$^{(*)}$, CIFAR-10$^{(\dagger)}$, SVHN$^{(*)}$, CelebA$^{(*)}$	UCI Regression Benchmark$^{(\dagger)}$, Sensorless Drive$^{(\dagger)}$, Bike Sharing$^{(\dagger)}$	Clusters (Synthetic), Univariate Regression (Synthetic))

C Fundamental Derivations Appendix

This appendix section walks the reader through generalized versions of recurring theoretical results using Dirichlet distributions in a Machine Learning context, such as their expectation in Appendix C.1, their entropy in Appendix C.2 and the Kullback-Leibler divergence between two Dirichlets in Appendix D.3.

C.1 Expectation of a Dirichlet

Here, we show results for the quantities $\mathbb{E}[\mu_k]$ and $\mathbb{E}[\log \mu_k]$. For the first, we follow the derivation by Miller (2011). Another proof is given by Lin (2016).

$$\mathbb{E}[\mu_k] = \int \cdots \int \mu_k \frac{\Gamma(\alpha_0)}{\prod_{k'=1}^{K} \Gamma(\alpha'_k)} \prod_{k'=1}^{K} \mu_{k'}^{\alpha_{k'}-1} d\mu_1 \dots d\mu_K \tag{30}$$

Moving $\mu_k^{\alpha_k - 1}$ out of the product:

$$= \int \cdots \int \frac{\Gamma(\alpha_0)}{\prod_{k'=1}^{K} \Gamma(\alpha_{k'})} \mu_k^{\alpha_k - 1 + 1} \prod_{k' \neq k} \mu_{k'}^{\alpha_{k'}-1} d\mu_1 \dots d\mu_K \tag{31}$$

For the next step, we define a new set of Dirichlet parameters with $\beta_k = \alpha_k + 1$ and $\forall k' \neq k : \beta_{k'} = \alpha_{k'}$. For those new parameters, $\beta_0 = \sum_k \beta_k = 1 + \alpha_0$. So by virtue of the Gamma function's property that $\Gamma(\beta_0) = \Gamma(\alpha_0 + 1) = \alpha_0 \Gamma(\alpha_0)$, replacing all terms in the normalization factor yields

$$= \int \cdots \int \frac{\alpha_k}{\alpha_0} \frac{\Gamma(\beta_0)}{\prod_{k'=1}^{K} \Gamma(\beta_{k'})} \prod_{k'=1}^{K} \mu_{k'}^{\beta_{k'}-1} d\mu_1 \dots d\mu_K = \frac{\alpha_k}{\alpha_0} \tag{32}$$

where in the last step we obtain the final result, since the Dirichlet with new parameters β_k must nevertheless integrate to 1, and the integrals do not regard α_k or α_0. For the expectation $\mathbb{E}[\log \mu_k]$, we first rephrase the Dirichlet distribution in terms of the exponential family (Kupperman, 1964). The exponential family encompasses many commonly-used distributions, such as the normal, exponential, Beta or Poisson, which all follow the form

$$p(\mathbf{x}; \boldsymbol{\eta}) = h(\mathbf{x}) \exp\left(\boldsymbol{\eta}^T u(\mathbf{x}) - A(\boldsymbol{\eta})\right) \tag{33}$$

with *natural parameters* $\boldsymbol{\eta}$, *sufficient statistic* $u(\mathbf{x})$, and *log-partition function* $A(\boldsymbol{\eta})$. For the Dirichlet distribution, Winn (2004) provides the sufficient statistic as $u(\boldsymbol{\mu}) = [\log \boldsymbol{\mu}_1, \dots, \boldsymbol{\mu}_K]^T$ and the log-partition function

$$A(\boldsymbol{\alpha}) = \sum_{k=1}^{K} \log \Gamma(\alpha_k) - \log \Gamma(\alpha_o) \tag{34}$$

By Mao (2019), we also find that by the moment-generating function that for the sufficient statistic, its expectation can be derived by

$$\mathbb{E}[u(\mathbf{x})_k] = \frac{\partial A(\boldsymbol{\eta})}{\partial \eta_k} \tag{35}$$

Therefore we can evaluate the expected value of $\log \mu_k$ (i.e. the sufficient statistic) by inserting the definition of the log-partition function in Equation (34) into Equation (35):

$$\mathbb{E}[\log \mu_k] = \frac{\partial}{\partial \alpha_k} \sum_{k=1}^{K} \log \Gamma(\alpha_k) - \log \Gamma(\alpha_0) = \psi(\alpha_k) - \psi(\alpha_0) \tag{36}$$

which corresponds precisely to the definition of the digamma function as $\psi(x) = \frac{d}{dx} \log \Gamma(x)$.

C.2 Entropy of Dirichlet

The following derivation is adapted from Lin (2016), with the result stated in Charpentier et al. (2020) as well.

$$\begin{aligned}
H[\boldsymbol{\mu}] &= -\mathbb{E}[\log p(\boldsymbol{\mu}|\boldsymbol{\alpha})] && (37)\\
&= -\mathbb{E}\left[\log\left(\frac{1}{B(\boldsymbol{\alpha})}\prod_{k=1}^{K}\mu_k^{\alpha_k-1}\right)\right] && (38)\\
&= -\mathbb{E}\left[-\log B(\boldsymbol{\alpha}) + \sum_{k=1}^{K}(\alpha_k-1)\log\mu_k\right] && (39)\\
&= \log B(\boldsymbol{\alpha}) - \sum_{k=1}^{K}(\alpha_k-1)\mathbb{E}[\log\mu_k] && (40)
\end{aligned}$$

Using Equation (36):

$$\begin{aligned}
&= \log B(\boldsymbol{\alpha}) - \sum_{k=1}^{K}(\alpha_k-1)\big(\psi(\alpha_k)-\psi(\alpha_0)\big) && (41)\\
&= \log B(\boldsymbol{\alpha}) + \sum_{k=1}^{K}(\alpha_k-1)\psi(\alpha_0) - \sum_{k=1}^{K}(\alpha_k-1)\psi(\alpha_k) && (42)\\
&= \log B(\boldsymbol{\alpha}) + (\alpha_0-K)\psi(\alpha_0) - \sum_{k=1}^{K}(\alpha_k-1)\psi(\alpha_k) && (43)
\end{aligned}$$

C.3 Kullback-Leibler Divergence between two Dirichlets

The following result is presented using an adapted derivation by Lin (2016) and appears in Chen et al. (2018) and Joo et al. (2020) as a starting point for their variational objective (see Appendix D.7). In the following we use $\mathrm{Dir}(\boldsymbol{\mu};\boldsymbol{\alpha})$ to denote the optimized distribution, and $\mathrm{Dir}(\boldsymbol{\mu};\boldsymbol{\gamma})$ the reference or target distribution.

$$\begin{aligned}
\mathrm{KL}\Big[p(\boldsymbol{\mu}|\boldsymbol{\alpha})\Big|\Big|p(\boldsymbol{\mu}|\boldsymbol{\gamma})\Big] =& \mathbb{E}\left[\log\frac{p(\boldsymbol{\mu}|\boldsymbol{\alpha})}{p(\boldsymbol{\mu}|\boldsymbol{\gamma})}\right] = \mathbb{E}\Big[\log p(\boldsymbol{\mu}|\boldsymbol{\alpha})\Big] - \mathbb{E}\Big[\log p(\boldsymbol{\mu}|\boldsymbol{\gamma})\Big] && (44)\\
=& \mathbb{E}\left[-\log B(\boldsymbol{\alpha}) + \sum_{k=1}^{K}(\alpha_k-1)\log\mu_k\right]\\
&-\mathbb{E}\left[-\log B(\boldsymbol{\gamma}) + \sum_{k=1}^{K}(\gamma_k-1)\log\mu_k\right] && (45)
\end{aligned}$$

Distributing and pulling out $B(\boldsymbol{\alpha})$ and $B(\boldsymbol{\gamma})$ out of the expectation (they don't depend on $\boldsymbol{\mu}$):

$$= -\log\frac{B(\boldsymbol{\gamma})}{B(\boldsymbol{\alpha})} + \mathbb{E}\left[\sum_{k=1}^{K}(\alpha_k-1)\log\mu_k - (\gamma_k-1)\log\mu_k\right] \tag{46}$$

$$= -\log \frac{B(\boldsymbol{\gamma})}{B(\boldsymbol{\alpha})} + \mathbb{E}\left[\sum_{k=1}^{K}(\alpha_k - \gamma_k)\log \mu_k\right] \tag{47}$$

Moving the expectation inward and using the identity $\mathbb{E}[\mu_k] = \psi(\alpha_k) - \psi(\alpha_0)$ from Appendix C.1:

$$= -\log \frac{B(\boldsymbol{\gamma})}{B(\boldsymbol{\alpha})} + \sum_{k=1}^{K}(\alpha_k - \gamma_k)\big(\psi(\alpha_k) - \psi(\alpha_0)\big) \tag{48}$$

The KL divergence is also used by some works as regularizer by penalizing the distance to a uniform Dirichlet with $\boldsymbol{\gamma} = \mathbf{1}$ (Sensoy et al., 2018). In this case, the result above can be derived to be

$$\mathrm{KL}\Big[p(\boldsymbol{\mu}|\boldsymbol{\alpha})\Big|\Big|p(\boldsymbol{\mu}|\mathbf{1})\Big] = \log \frac{\Gamma(K)}{B(\boldsymbol{\alpha})} + \sum_{k=1}^{K}(\alpha_k - 1)\big(\psi(\alpha_k) - \psi(\alpha_0)\big) \tag{49}$$

where the $\log \Gamma(K)$ term can also be omitted for optimization purposes, since it does not depend on $\boldsymbol{\alpha}$.

D Additional Derivations Appendix

In this appendix we present relevant results in a Machine Learning context, including from some of the surveyed works, featuring as unified notation and annotated derivation steps. These include derivations of expected entropy (Appendix D.1) and mutual information (Appendix D.2) as uncertainty metrics for Dirichlet networks. Also, we derive a multitude of loss functions, including the l_∞ norm loss of a Dirichlet w.r.t. a one-hot encoded class label in Appendix D.3, the l_2 norm loss in Appendix D.4, as well as the reverse KL loss by Malinin & Gales (2019), the UCE objective Biloš et al. (2019); Charpentier et al. (2020) and ELBO Shen et al. (2020); Chen et al. (2018) as training objectives (Appendices D.5 to D.7).

D.1 Derivation of Expected Entropy

The following derivation is adapted from Malinin & Gales (2018) appendix section C.4. In the following, we assume that $\forall k \in \mathbb{K} : \mu_k > 0$:

$$\mathbb{E}_{p(\boldsymbol{\mu}|\,\mathbf{x},\hat{\boldsymbol{\theta}})}\Big[H\Big[P(y|\boldsymbol{\mu})\Big]\Big] = \int p(\boldsymbol{\mu}|\,\mathbf{x},\hat{\boldsymbol{\theta}})\Big(-\sum_{k=1}^{K}\mu_k\log\mu_k\Big)d\boldsymbol{\mu} \tag{50}$$

$$= -\sum_{k=1}^{K}\int p(\boldsymbol{\mu}|\,\mathbf{x},\hat{\boldsymbol{\theta}})\Big(\mu_k\log\mu_k\Big)d\boldsymbol{\mu} \tag{51}$$

Inserting the definition of $p(\boldsymbol{\mu}|\,\mathbf{x},\hat{\boldsymbol{\theta}}) \approx p(\boldsymbol{\mu}|\,\mathbf{x},\mathbb{D})$:

$$= -\sum_{k=1}^{K}\left(\frac{\Gamma(\alpha_0)}{\prod_{k'=1}^{K}\Gamma(\alpha_{k'})}\int \mu_k\log\mu_k\prod_{k'=1}^{K}\mu_{k'}^{\alpha_{k'}-1}d\boldsymbol{\mu}\right) \tag{52}$$

Singling out the factor μ_k:

$$= -\sum_{k=1}^{K}\left(\frac{\Gamma(\alpha_0)}{\Gamma(\alpha_k)\prod_{k'\neq k}\Gamma(\alpha_{k'})}\mu_k^{\alpha_k-1}\int \mu_k\log\mu_k\prod_{k'\neq k}\mu_{k'}^{\alpha_{k'}-1}d\boldsymbol{\mu}\right) \tag{53}$$

Adjusting the normalizing constant (this is the same trick used in Appendix C.1):

$$= -\sum_{k=1}^{K}\left(\frac{\alpha_k}{\alpha_0}\int \frac{\Gamma(\alpha_0+1)}{\Gamma(\alpha_k+1)\prod_{k'\neq k}\Gamma(\alpha_{k'})}\mu_k^{\alpha_k-1}\log\mu_k\prod_{k'\neq k}\mu_{k'}^{\alpha_{k'}-1}d\boldsymbol{\mu}\right) \tag{54}$$

Using the identity $\mathbb{E}[\log\mu_k] = \psi(\alpha_k) - \psi(\alpha_0)$ (Equation (36)). Since the expectation here is w.r.t to a Dirichlet with concentration parameters $\alpha_k + 1$, we obtain

$$= -\sum_{k=1}^{K}\frac{\alpha_k}{\alpha_0}\Big(\psi(\alpha_k+1) - \psi(\alpha_0+1)\Big) \tag{55}$$

D.2 Derivation of Mutual Information

We start from the expression in Equation (13):

$$I\Big[y,\boldsymbol{\mu}\Big|\,\mathbf{x},\mathbb{D}\Big] = H\Big[\mathbb{E}_{p(\boldsymbol{\mu}|\,\mathbf{x},\mathbb{D})}\Big[P(y|\boldsymbol{\mu})\Big]\Big] - \mathbb{E}_{p(\boldsymbol{\mu}|\,\mathbf{x},\mathbb{D})}\Big[H\Big[P(y|\boldsymbol{\mu})\Big]\Big] \tag{56}$$

Given that $\mathbb{E}[\mu_k] = \frac{\alpha_k}{\alpha_0}$ (Appendix C.1) and assuming that point estimate $p(\boldsymbol{\mu}|\,\mathbf{x}, \mathbb{D}) \approx p(\boldsymbol{\mu}|\,\mathbf{x}, \hat{\boldsymbol{\theta}})$ is sufficient (Malinin & Gales, 2018), we can identify the first term as the Shannon entropy $-\sum_{k=1}^{K} \mu_k \log \mu_k = -\sum_{k=1}^{K} \frac{\alpha_k}{\alpha_0} \log \frac{\alpha_k}{\alpha_0}$. Furthermore, the second part we already derived in Appendix D.1 and thus we obtain:

$$= -\sum_{k=1}^{K} \frac{\alpha_k}{\alpha_0} \log \frac{\alpha_k}{\alpha_0} + \sum_{k=1}^{K} \frac{\alpha_k}{\alpha_0} \Big(\psi(\alpha_k + 1) - \psi(\alpha_0 + 1) \Big) \tag{57}$$

$$= -\sum_{k=1}^{K} \frac{\alpha_k}{\alpha_0} \Big(\log \frac{\alpha_k}{\alpha_0} - \psi(\alpha_k + 1) + \psi(\alpha_0 + 1) \Big) \tag{58}$$

D.3 l_∞ Norm Derivation

In this section we elaborate on the derivation of Tsiligkaridis (2019) deriving a generalized l_p loss, upper-bounding the l_∞ loss. This in turn allows us to easily derive the l_2 loss used by Sensoy et al. (2018); Zhao et al. (2020). Here we assume the classification target y is provided in the form of a one-hot encoded label $\mathbf{y} = [\mathbf{1}_{y=1}, \ldots, \mathbf{1}_{y=K}]^T$.

$$\mathbb{E}_{p(\boldsymbol{\mu}|\,\mathbf{x},\boldsymbol{\theta})} \big[||\,\mathbf{y} - \boldsymbol{\mu}||_\infty \big] \leq \mathbb{E}_{p(\boldsymbol{\mu}|\,\mathbf{x},\boldsymbol{\theta})} \big[||\,\mathbf{y} - \boldsymbol{\mu}||_p \big] \tag{59}$$

Using Jensen's inequality

$$\leq \Big(\mathbb{E}_{p(\boldsymbol{\mu}|\,\mathbf{x},\boldsymbol{\theta})} \big[||\,\mathbf{y} - \boldsymbol{\mu}||_p^p \big] \Big)^{1/p} \tag{60}$$

Evaluating the expression with $\forall k \neq y : \mathbf{y}_k = 0$:

$$= \Big(\mathbb{E}[(1 - \mu_y)^p] + \sum_{k \neq y} \mathbb{E}[\mu_k^p] \Big)^{1/p} \tag{61}$$

In order to compute the expression above, we first realize that all components of μ are distributed according to a Beta distribution $\text{Beta}(\alpha, \beta)$ (since the Dirichlet is a multivariate generalization of the beta distribution) for which the moment-generating function is given as follows:

$$\mathbb{E}[\mu^p] = \frac{\Gamma(\alpha + p)\Gamma(\beta)\Gamma(\alpha + \beta)}{\Gamma(\alpha + p + \beta)\Gamma(\alpha)\Gamma(\beta)} = \frac{\Gamma(\alpha + p)\Gamma(\alpha + \beta)}{\Gamma(\alpha + p + \beta)\Gamma(\alpha)} \tag{62}$$

Given that the first term in Equation (59) is characterized by $\text{Beta}(\alpha_0 - \alpha_y, \alpha_y)$ and the second one by $\text{Beta}(\alpha_k, \alpha_0 - \alpha_k)$, we can evaluate the result in Equation (59) using the moment generating function:

$$\mathbb{E}_{p(\boldsymbol{\mu}|\,\mathbf{x},\boldsymbol{\theta})} \Big[||\,\mathbf{y} - \boldsymbol{\mu}||_\infty \Big] \leq \left(\frac{\Gamma(\alpha_0 - \alpha_y + p)\Gamma(\alpha_0 - \cancel{\alpha_y} + \cancel{\alpha_y})}{\Gamma(\alpha_0 - \cancel{\alpha_y} + p + \cancel{\alpha_y})\Gamma(\alpha_0 - \alpha_y)} + \sum_{k \neq y} \frac{\Gamma(\alpha_k + p)\Gamma(\cancel{\alpha_k} + \alpha_0 - \cancel{\alpha_k})}{\Gamma(\cancel{\alpha_k} + p + \alpha_0 - \cancel{\alpha_k})\Gamma(\alpha_k)} \right)^{\frac{1}{p}} \tag{63}$$

$$= \left(\frac{\Gamma(\alpha_0 - \alpha_y + p)\Gamma(\alpha_0)}{\Gamma(\alpha_0 + p)\Gamma(\alpha_0 - \alpha_y)} + \sum_{k \neq y} \frac{\Gamma(\alpha_k + p)\Gamma(\alpha_0)}{\Gamma(p + \alpha_0)\Gamma(\alpha_k)} \right)^{\frac{1}{p}} \tag{64}$$

Factoring out common terms:

$$= \left(\frac{\Gamma(\alpha_0)}{\Gamma(\alpha_0 + p)} \left(\frac{\Gamma(\alpha_0 - \alpha_y + p)}{\Gamma(\alpha_0 - \alpha_y)} + \sum_{k \neq y} \frac{\Gamma(\alpha_k + p)}{\Gamma(\alpha_k)} \right) \right)^{\frac{1}{p}} \tag{65}$$

Expressing $\alpha_0 - \alpha_k = \sum_{k \neq y} \alpha_k$:

$$= \left(\frac{\Gamma(\alpha_0)}{\Gamma(\alpha_0 + p)} \right)^{\frac{1}{p}} \left(\frac{\Gamma\Big(\sum_{k \neq y} \alpha_k + p \Big)}{\Gamma\Big(\sum_{k \neq y} \alpha_k \Big)} + \sum_{k \neq y} \frac{\Gamma(\alpha_k + p)}{\Gamma(\alpha_k)} \right)^{\frac{1}{p}} \tag{66}$$

D.4 l_2 Norm Loss Derivation

Here we present an adapted derivation by Sensoy et al. (2018) for the l_2-norm loss to train Dirichlet networks. Here we again use a one-hot vector for a label with $\mathbf{y} = [\mathbf{1}_{y=1}, \ldots, \mathbf{1}_{y=K}]^T$.

$$\mathbb{E}_{p(\boldsymbol{\mu}|\,\mathbf{x},\boldsymbol{\theta})} \Big[||\,\mathbf{y} - \boldsymbol{\mu}||_2^2 \Big] = \mathbb{E} \Big[\sum_{k=1}^{K} (\mathbf{1}_{y=k} - \mu_k)^2 \Big] \tag{67}$$

$$= \mathbb{E} \Big[\sum_{k=1}^{K} \mathbf{1}_{y=k}^2 - 2\mu_k \mathbf{1}_{y=k} + \mu_k^2 \Big] \tag{68}$$

$$= \sum_{k=1}^{K} \mathbf{1}_{y=k}^2 - 2\mathbb{E}[\mu_k]\mathbf{1}_{y=k} + \mathbb{E}[\mu_k^2] \tag{69}$$

Using the identity that $\mathbb{E}[\mu_k^2] = \mathbb{E}[\mu_k]^2 + \mathrm{Var}(\mu_k)$:

$$= \sum_{k=1}^{K} \mathbf{1}_{y=k}^2 - 2\mathbb{E}[\mu_k]\mathbf{1}_{y=k} + \mathbb{E}[\mu_k]^2 + \mathrm{Var}(\mu_k) \tag{70}$$

$$= \sum_{k=1}^{K} \Big(\mathbf{1}_{y=k} - \mathbb{E}[\mu_k] \Big)^2 + \mathrm{Var}(\mu_k) \tag{71}$$

Finally, we use the result from Appendix C.1 and the result that $\mathrm{Var}(\mu_k) = \dfrac{\alpha_k(\alpha_0 - \alpha_k)}{\alpha_0^2(\alpha_0 + 1)}$ (see Lin, 2016):

$$= \sum_{k=1}^{K} \Big(\mathbf{1}_{y=k} - \frac{\alpha_k}{\alpha_0} \Big)^2 + \frac{\alpha_k(\alpha_0 - \alpha_k)}{\alpha_0^2(\alpha_0 + 1)} \tag{72}$$

D.5 Derivation of Reverse KL loss

Here we re-state and annotate the derivation of reverse KL loss by Malinin & Gales (2019) in more detail, starting from the forward KL loss by Malinin & Gales (2018). Note that here, $\hat{\boldsymbol{\alpha}}$ contains a dependence on k, since Malinin & Gales (2018) let $\hat{\alpha}_k = \hat{\mu}_k \hat{\alpha}_0$ with $\hat{\alpha}_0$ being a hyperparameter and $\hat{\mu}_k = \mathbf{1}_{k=y} + (-\mathbf{1}_{k=y}K + 1)\varepsilon$ and ε being a small number.

$$\mathbb{E}_{p(\mathbf{x},y)} \Big[\sum_{k=1}^{K} \mathbf{1}_{y=k} \mathrm{KL} \Big[p(\boldsymbol{\mu}|\hat{\boldsymbol{\alpha}}) \Big| \Big| p(\boldsymbol{\mu}|\,\mathbf{x}, \boldsymbol{\theta}) \Big] \Big] \tag{73}$$

$$= \mathbb{E}_{p(\mathbf{x},y)} \Big[\sum_{k=1}^{K} \mathbf{1}_{y=k} \int p(\boldsymbol{\mu}|\hat{\boldsymbol{\alpha}}) \log \frac{p(\boldsymbol{\mu}|\hat{\boldsymbol{\alpha}})}{p(\boldsymbol{\mu}|\,\mathbf{x}, \boldsymbol{\theta})} d\boldsymbol{\mu} \Big] \tag{74}$$

Writing the expectation explicitly:

$$= \int \sum_{k=1}^{K} p(y = k, \mathbf{x}) \sum_{k=1}^{K} \mathbf{1}_{y=k} \int p(\boldsymbol{\mu}|\hat{\boldsymbol{\alpha}}) \log \frac{p(\boldsymbol{\mu}|\hat{\boldsymbol{\alpha}})}{p(\boldsymbol{\mu}|\,\mathbf{x}, \boldsymbol{\theta})} d\boldsymbol{\mu} d\,\mathbf{x} \tag{75}$$

$$= \int \sum_{k=1}^{K} p(\mathbf{x}) P(y=k|\,\mathbf{x}) \sum_{k=1}^{K} \mathbf{1}_{y=k} \int p(\boldsymbol{\mu}|\hat{\boldsymbol{\alpha}}) \log \frac{p(\boldsymbol{\mu}|\hat{\boldsymbol{\alpha}})}{p(\boldsymbol{\mu}|\,\mathbf{x},\boldsymbol{\theta})} d\boldsymbol{\mu} d\,\mathbf{x} \tag{76}$$

$$= \mathbb{E}_{p(\mathbf{x})} \left[\sum_{k=1}^{K} P(y=k|\,\mathbf{x}) \sum_{k=1}^{K} \mathbf{1}_{y=k} \int p(\boldsymbol{\mu}|\hat{\boldsymbol{\alpha}}) \log \frac{p(\boldsymbol{\mu}|\hat{\boldsymbol{\alpha}})}{p(\boldsymbol{\mu}|\,\mathbf{x},\boldsymbol{\theta})} d\boldsymbol{\mu} \right] \tag{77}$$

Adding factor in log, collapsing double sum:

$$= \mathbb{E}_{p(\mathbf{x})} \left[\sum_{k=1}^{K} P(y=k|\,\mathbf{x}) \int p(\boldsymbol{\mu}|\hat{\boldsymbol{\alpha}}) \log \left(\frac{p(\boldsymbol{\mu}|\hat{\boldsymbol{\alpha}}) \sum_{k=1}^{K} P(y=k|\,\mathbf{x})}{p(\boldsymbol{\mu}|\,\mathbf{x},\boldsymbol{\theta}) \sum_{k=1}^{K} P(y=k|\,\mathbf{x})} \right) d\boldsymbol{\mu} \right] \tag{78}$$

Reordering, separating constant factor from log:

$$= \mathbb{E}_{p(\mathbf{x})} \left[\int \sum_{k=1}^{K} P(y=k|\,\mathbf{x}) p(\boldsymbol{\mu}|\hat{\boldsymbol{\alpha}}) \left(\log \left(\frac{\sum_{k=1}^{K} P(y=k|\,\mathbf{x}) p(\boldsymbol{\mu}|\hat{\boldsymbol{\alpha}})}{p(\boldsymbol{\mu}|\,\mathbf{x},\boldsymbol{\theta})} \right) \right. \right. \tag{79}$$

$$\left. \left. \underbrace{- \log \left(\sum_{k=1}^{K} P(y=k|\,\mathbf{x}) \right)}_{=0} \right) d\boldsymbol{\mu} \right] \tag{80}$$

$$= \mathbb{E}_{p(\mathbf{x})} \left[\mathrm{KL} \left[\underbrace{\sum_{k=1}^{K} P(y=k|\,\mathbf{x}) p(\boldsymbol{\mu}|\hat{\alpha})}_{\text{Mixture of } K \text{ Dirichlets}} \middle| \middle| p(\boldsymbol{\mu}|\,\mathbf{x},\boldsymbol{\theta}) \right] \right] \tag{81}$$

where we can see that this objective actually tries to minimizes the divergence towards a mixture of K Dirichlet distributions. In the case of high data uncertainty, this is claimed incentivize the model to distribute mass around each of the corners of the simplex, instead of the desired behavior shown in Figure 4c. Therefore, Malinin & Gales (2019) propose to swap the order of arguments in the KL-divergence, resulting in the following:

$$\mathbb{E}_{p(\mathbf{x})} \left[\sum_{k=1}^{K} P(y=k|\,\mathbf{x}) \cdot \mathrm{KL} \Big[p(\boldsymbol{\mu}|\,\mathbf{x},\boldsymbol{\theta}) \Big| \Big| p(\boldsymbol{\mu}|\hat{\boldsymbol{\alpha}}) \Big] \right] \tag{82}$$

$$= \mathbb{E}_{p(\mathbf{x})} \left[\sum_{k=1}^{K} p(y=k|\,\mathbf{x}) \cdot \int p(\boldsymbol{\mu}|\,\mathbf{x},\boldsymbol{\theta}) \log \frac{p(\boldsymbol{\mu}|\,\mathbf{x},\boldsymbol{\theta})}{p(\boldsymbol{\mu}|\hat{\boldsymbol{\alpha}})} d\boldsymbol{\mu} \right] \tag{83}$$

Reordering:

$$= \mathbb{E}_{p(\mathbf{x})} \left[\int p(\boldsymbol{\mu}|\,\mathbf{x},\boldsymbol{\theta}) \sum_{k=1}^{K} P(y=k|\,\mathbf{x}) \log \frac{p(\boldsymbol{\mu}|\,\mathbf{x},\boldsymbol{\theta})}{p(\boldsymbol{\mu}|\hat{\boldsymbol{\alpha}})} d\boldsymbol{\mu} \right] \tag{84}$$

$$= \mathbb{E}_{p(\mathbf{x})} \left[\mathbb{E}_{p(\boldsymbol{\mu}|\,\mathbf{x},\boldsymbol{\theta})} \left[\sum_{k=1}^{K} P(y=k|\,\mathbf{x}) \log p(\boldsymbol{\mu}|\,\mathbf{x},\boldsymbol{\theta}) - \sum_{k=1}^{K} P(y=k|\,\mathbf{x}) \log p(\boldsymbol{\mu}|\hat{\boldsymbol{\alpha}}) \right] \right] \tag{85}$$

$$= \mathbb{E}_{p(\mathbf{x})} \left[\int p(\boldsymbol{\mu}|\,\mathbf{x},\boldsymbol{\theta}) \left(\log \left(\prod_{k=1}^{K} p(\boldsymbol{\mu}|\,\mathbf{x},\boldsymbol{\theta})^{P(y=k|\,\mathbf{x})} \right) - \log \left(\prod_{k=1}^{K} p(\boldsymbol{\mu}|\hat{\boldsymbol{\alpha}})^{P(y=k|\,\mathbf{x})} \right) \right) d\boldsymbol{\mu} \right] \tag{86}$$

$$= \mathbb{E}_{p(\mathbf{x})} \left[\int p(\boldsymbol{\mu}|\,\mathbf{x},\boldsymbol{\theta}) \left(\log \left(p(\boldsymbol{\mu}|\,\mathbf{x},\boldsymbol{\theta})^{\sum_{k=1}^{K} P(y=k|\,\mathbf{x})} \right) \right. \right. \tag{87}$$

$$\left. \left. - \log \left(\prod_{k=1}^{K} \left(\frac{1}{B(\boldsymbol{\alpha})} \prod_{k'=1}^{K} \mu_{k'}^{\alpha_{k'}-1} \right)^{p(y=k|\,\mathbf{x})} \right) \right) d\boldsymbol{\mu} \right] \tag{88}$$

$$= \mathbb{E}_{p(\mathbf{x})}\left[\int p(\boldsymbol{\mu}|\,\mathbf{x},\boldsymbol{\theta})\Big(\log\big(p(\boldsymbol{\mu}|\,\mathbf{x},\boldsymbol{\theta})\big) - \log\Big(\prod_{k=1}^{K}\Big(\frac{1}{B(\boldsymbol{\alpha})}\prod_{k'=1}^{K}\mu_{k'}^{\alpha_{k'}-1}\Big)^{P(y=k|\,\mathbf{x})}\Big)d\boldsymbol{\mu}\right] \tag{89}$$

$$= \mathbb{E}_{p(\mathbf{x})}\left[\int p(\boldsymbol{\mu}|\,\mathbf{x},\boldsymbol{\theta})\Big(\log\big(p(\boldsymbol{\mu}|\,\mathbf{x},\boldsymbol{\theta})\big) - \log\Big(\frac{1}{B(\boldsymbol{\alpha})}\prod_{k'=1}^{K}\mu_{k'}^{\sum_{k=1}^{K}P(y=k|\,\mathbf{x})\alpha_{k'}-1}\Big)d\boldsymbol{\mu}\right] \tag{90}$$

$$= \mathbb{E}_{p(\mathbf{x})}\Big[\mathrm{KL}\Big[p(\boldsymbol{\mu}|\,\mathbf{x},\boldsymbol{\theta})||p(\boldsymbol{\mu}|\bar{\boldsymbol{\alpha}})\Big]\Big] \quad \text{where} \quad \bar{\boldsymbol{\alpha}} = \sum_{k=1}^{K}p(y=k|\,\mathbf{x})\alpha_{k'} \tag{91}$$

Therefore, instead of a mixture of Dirichlet distribution, we obtain a single distribution whose *parameters are a mixture* of the concentrations of each class.

D.6 Uncertainty-aware Cross-Entropy Loss

The uncertainty-aware cross-entropy loss in Biloš et al. (2019); Charpentier et al. (2020) has the form

$$\mathcal{L}_{\mathrm{UCE}} = \mathbb{E}_{p(\boldsymbol{\mu}|\,\mathbf{x},\boldsymbol{\theta})}[\log p(y|\boldsymbol{\mu})] = \mathbb{E}[\log \mu_y] = \psi(\alpha_y) - \psi(\alpha_0) \tag{92}$$

as $p(y|\boldsymbol{\mu})$ is given by the true label in form of a delta distribution, we can apply the result from Appendix C.1.

D.7 Evidence-Lower Bound For Dirichlet Posterior Estimation

The evidence lower bound is a well-known objective to optimize the KL-divergence between an approximate proposal and target distribution (Jordan et al., 1999; Kingma & Welling, 2014). We derive it based on Chen et al. (2018) in the following for the Dirichlet case with a proposal distribution $p(\boldsymbol{\mu}|\,\mathbf{x},\boldsymbol{\theta})$ to the target distribution $p(\boldsymbol{\mu}|y)$. For the first part of the derivation, we omit the dependence on $\boldsymbol{\beta}$ for clarity.

$$\mathrm{KL}\big[p(\boldsymbol{\mu}|\,\mathbf{x},\boldsymbol{\theta})\big|\big|p(\boldsymbol{\mu}|y)\big] = \mathbb{E}_{p(\boldsymbol{\mu}|\,\mathbf{x},\boldsymbol{\theta})}\left[\log\frac{p(\boldsymbol{\mu}|\,\mathbf{x},\boldsymbol{\theta})}{p(\boldsymbol{\mu}|y)}\right] = \mathbb{E}_{p(\boldsymbol{\mu}|\,\mathbf{x},\boldsymbol{\theta})}\left[\log\frac{p(\boldsymbol{\mu}|\,\mathbf{x},\boldsymbol{\theta})p(y)}{p(\boldsymbol{\mu},y)}\right] \tag{93}$$

Factorizing $p(\boldsymbol{\mu},y) = P(y|\boldsymbol{\mu})p(\boldsymbol{\mu})$, pulling out $p(y)$ as it doesn't depend on μ:

$$= \mathbb{E}_{p(\boldsymbol{\mu}|\,\mathbf{x},\boldsymbol{\theta})}\left[\log\frac{p(\boldsymbol{\mu}|\,\mathbf{x},\boldsymbol{\theta})}{P(y|\boldsymbol{\mu})p(\boldsymbol{\mu})}\right] + p(y) \tag{94}$$

$$= \mathbb{E}_{p(\boldsymbol{\mu}|\,\mathbf{x},\boldsymbol{\theta})}\left[\log\frac{p(\boldsymbol{\mu}|\,\mathbf{x},\boldsymbol{\theta})}{p(\boldsymbol{\mu})}\right] - \mathbb{E}_{p(\boldsymbol{\mu}|\,\mathbf{x},\boldsymbol{\theta})}\big[\log P(y|\boldsymbol{\mu})\big] + p(y) \tag{95}$$

$$\leq \mathrm{KL}\big[p(\boldsymbol{\mu}|\,\mathbf{x},\boldsymbol{\theta})\big|\big|p(\boldsymbol{\mu})\big] - \mathbb{E}_{p(\boldsymbol{\mu}|\,\mathbf{x},\boldsymbol{\theta})}\big[\log P(y|\boldsymbol{\mu})\big] \tag{96}$$

Now note that the second part of the result is the uncertainty-aware cross-entropy loss from Appendix D.6 and re-adding the dependence of $p(\mu)$ on $\boldsymbol{\gamma}$, we can re-use our result regarding the KL-divergence between two Dirichlets in Appendix C.3 and thus obtain:

$$\mathcal{L}_{\mathrm{ELBO}} = \psi(\beta_y) - \psi(\beta_0) - \log\frac{B(\boldsymbol{\beta})}{B(\boldsymbol{\gamma})} + \sum_{k=1}^{K}(\beta_k - \gamma_k)\big(\psi(\beta_k) - \psi(\beta_0)\big) \tag{97}$$

which is exactly the solution obtained by both Chen et al. (2018) and Joo et al. (2020).

E Overview over Loss Functions Appendix

In Tables 6 and 7, we compare the forms of the loss function used by Evidential Deep Learning methods for classification, using the consistent notation from the paper. Most of the presented results can be found in the previous Appendix C and Appendix D. We refer to the original work for details about the objective of Nandy et al. (2020).

Table 6: Overview over objectives used by prior networks for classification.

Method	Loss function	Regularizer	Comment
Prior networks (Malinin & Gales, 2018)	$\log \frac{B(\hat{\boldsymbol{\alpha}})}{B(\boldsymbol{\alpha})} + \sum_{k=1}^{K}(\alpha_k - \hat{\alpha}_k)\big(\psi(\alpha_k) - \psi(\alpha_0)\big)$	$-\log \frac{\Gamma(K)}{B(\boldsymbol{\alpha})} + \sum_{k=1}^{K}(\alpha_k - 1)(\psi(\alpha_k) - \psi(\alpha_0))$	Target concentration parameters $\hat{\boldsymbol{\alpha}}$ are created using a label smoothing approach, i.e. $\hat{\mu}_k = \begin{cases} 1-(K-1)\varepsilon & \text{if } y = k \\ \varepsilon & \text{if } y \neq k \end{cases}$. Together with setting $\hat{\alpha}_0$ as a hyperparameter, $\hat{\alpha}_k = \hat{\mu}_k \hat{\alpha}_0$
Prior networks (Malinin & Gales, 2019)	$\log \frac{B(\hat{\boldsymbol{\alpha}})}{B(\boldsymbol{\alpha})} + \sum_{k=1}^{K}(\alpha_k - \hat{\alpha}_k)\big(\psi(\alpha_k) - \psi(\alpha_0)\big)$	$\log \frac{B(\bar{\boldsymbol{\alpha}})}{B(\boldsymbol{\alpha})} + \sum_{k=1}^{K}(\alpha_k - \bar{\alpha}_k)\big(\psi(\alpha_k) - \psi(\alpha_0)\big)$	Similar to above, $\hat{\alpha}_c^{(k)} = \mathbf{1}_{c=k}\alpha_{\text{in}} + 1$ for in-distribution and $\bar{\alpha}_c^{(k)} = \mathbf{1}_{c=k}\alpha_{\text{out}} + 1$ where we have hyperparameters set to $\alpha_{\text{in}} = 0.01$ and $\alpha_{\text{out}} = 0$. Then finally, $\hat{\boldsymbol{\alpha}} = \sum_{k=1}^{K} p(y=k\|\mathbf{x})\hat{\alpha}_k$ and $\bar{\boldsymbol{\alpha}} = \sum_{k=1}^{K} p(y=k\|\mathbf{x})\bar{\alpha}_k$.
Information Robust Dirichlet Networks (Tsiligkaridis, 2019)	$\left(\frac{\Gamma(\alpha_0)}{\Gamma(\alpha_0+p)}\right)^{\frac{1}{p}} \left(\frac{\Gamma\left(\sum_{k\neq y}\alpha_k + p\right)}{\Gamma\left(\sum_{k\neq y}\alpha_k\right)} + \sum_{k\neq y}\frac{\Gamma(\alpha_k+p)}{\Gamma(\alpha_k)}\right)^{\frac{1}{p}}$	$\frac{1}{2}\sum_{k\neq y}(\alpha_k - 1)^2(\psi^{(1)}(\alpha_k) - \psi^{(1)})(\alpha_0))$	$\psi^{(1)}$ is the polygamma function defined as $\psi^{(1)}(x) = \frac{d}{dx}\psi(x)$.
Dirichlet via Function Decomposition (Biloš et al., 2019)	$\psi(\alpha_y) - \psi(\alpha_0)$	$\lambda_1 \int_0^T \mu_k(\tau)^2 d\tau + \lambda_2 \int_0^T (\nu - \sigma^2(\tau))^2 d\tau$	Factors λ_1 and λ_2 that are treated as hyperparameters that weigh first term pushing the for logit k to zero, while pushing the variance in the first term to ν.
Prior network with PAC Reg. (Haussmann et al., 2019)	$-\log \mathbb{E}\left[\prod_{k=1}^{K}\left(\frac{\alpha_k}{\alpha_0}\right)^{\mathbf{1}_{k=y}}\right]$	$\sqrt{\frac{\text{KL}\left[p(\boldsymbol{\mu}\|\boldsymbol{\alpha})\middle\|p(\boldsymbol{\mu}\|\mathbf{1})\right] - \log\delta}{N}} - 1$	The expectation in the loss function is evaluated using parameter samples from a weight distribution. $\delta \in [0,1]$.
Ensemble Distribution Distillation (Malinin et al., 2020b)	$\psi(\alpha_0) - \sum_{k=1}^{K}\psi(\alpha_k) + \frac{1}{M}\sum_{m=1}^{M}\sum_{k=1}^{K}(\alpha_k - 1)$ $\log p(y=k\|\mathbf{x}, \boldsymbol{\theta}^{(m)})$	-	The objective uses predictions from a trained ensemble with parameters $\boldsymbol{\theta}_1, \ldots, \boldsymbol{\theta}_M$.
Prior networks with representation gap (Nandy et al., 2020)	$-\log \mu_y - \frac{\lambda_{\text{in}}}{K}\sum_{k=1}^{K}\sigma(\alpha_k)$	$-\sum_{k=1}\frac{1}{K}\log\mu_k - \frac{\lambda_{\text{out}}}{K}\sum_{k=1}^{K}\sigma(\alpha_k)$	The main objective is being optimized on in-distribution, the regularizer on out-of-distribution data. λ_{in} and λ_{out} weighing terms and σ denotes the sigmoid function.
Prior RNN (Shen et al., 2020)	$\sum_{k=1}\mathbf{1}_{k=y}\log\mu_k$	$-\log B(\tilde{\boldsymbol{\alpha}}) + (\hat{\alpha}_0 - K)\psi(\hat{\alpha}_0) - \sum_{k=1}^{K}(\hat{\alpha}_k - 1)\psi(\hat{\alpha}_k)$	Here, the entropy regularizer operates on a scaled version of the concentration parameters $\tilde{\boldsymbol{\alpha}} = (\mathbf{I}_K - \mathbf{W})\boldsymbol{\alpha}$, where $\mathbf{W}$ is learned.
Graph-based Kernel Dirichlet dist. est. (GKDE) (Zhao et al., 2020)	$\sum_{k=1}^{K}\left(\mathbf{1}_{y=k} - \frac{\alpha_k}{\alpha_0}\right)^2 + \frac{\alpha_k(\alpha_0-\alpha_k)}{\alpha_0^2(\alpha_0+1)}$	$-\log\frac{B(\boldsymbol{\alpha})}{B(\hat{\boldsymbol{\alpha}})} + \sum_{k=1}^{K}(\alpha_k - \hat{\alpha}_k)\big(\psi(\alpha_k) - \psi(\alpha_0)\big)$	$\hat{\boldsymbol{\alpha}}$ here corresponds to a uniform prior including some information about the local graph structure. The authors also use an additional knowledge distillation objective, which was omitted here since it doesn't related to the Dirichlet.

Table 7: Overview over objectives used by posterior networks for classification.

Method	Loss function	Regularizer	Comment
Evidential Deep Learning (Sensoy et al., 2018)	$\sum_{k=1}^{K}\left(\mathbf{1}_{y=k}-\frac{\beta_k}{\beta_0}\right)^2+\frac{\beta_k(\beta_0-\beta_k)}{\beta_0^2(\beta_0+1)}$	$-\log\frac{\Gamma(K)}{B(\boldsymbol{\beta})}+\sum_{k=1}^{K}(\beta_k-1)\big(\psi(\beta_k)-\psi(\beta_0)\big)$	
Variational Dirichlet (Chen et al., 2018)	$\psi(\beta_y)-\psi(\beta_0)$	$-\log\frac{B(\boldsymbol{\beta})}{B(\boldsymbol{\gamma})}+\sum_{k=1}^{K}(\beta_k-\gamma_k)\big(\psi(\beta_k)-\psi(\beta_0)\big)$	
Regularized ENN Zhao et al. (2019)	$\sum_{k=1}^{K}\left(\mathbf{1}_{y=k}-\frac{\beta_k}{\beta_0}\right)^2+\frac{\beta_k(\beta_0-\beta_k)}{\beta_0^2(\beta_0+1)}$	$-\lambda_1\mathbb{E}_{p_{\text{out}}(\mathbf{x},y)}\left[\frac{\alpha_y}{\alpha_0}\right]-\lambda_2\mathbb{E}_{p_{\text{confl.}}(\mathbf{x},y)}\left[\sum_{k=1}^{K}\left(\frac{\beta_k\sum_{k'\neq k}\beta_{k'}\left(1-\frac{\lvert\beta_{k'}-\beta_k\rvert}{\beta_{k'}+\beta_k}\right)}{\sum_{k'\neq k}\beta_{k'}}\right)\right]$	The first term represents *vacuity*, i.e. the lack of evidence and is optimized using OOD examples. The second term stands for *dissonance*, and is computed using points with neighborhoods with different classes from their own. λ_1, λ_2 are hyperparameters.
WGAN–ENN (Hu et al., 2021)	$\sum_{k=1}^{K}\left(\mathbf{1}_{y=k}-\frac{\beta_k}{\beta_0}\right)^2+\frac{\beta_k(\beta_0-\beta_k)}{\beta_0^2(\beta_0+1)}$	$-\lambda\mathbb{E}_{p_{\text{out}}(\mathbf{x},y)}\left[\frac{\alpha_y}{\alpha_0}\right]$	
Belief Matching (Joo et al., 2020)	$\psi(\beta_y)-\psi(\beta_0)$	$-\log\frac{B(\boldsymbol{\beta})}{B(\boldsymbol{\gamma})}+\sum_{k=1}^{K}(\beta_k-\gamma_k)\big(\psi(\beta_k)-\psi(\beta_0)\big)$	
Posterior networks (Charpentier et al., 2020)	$\psi(\beta_y)-\psi(\beta_0)$	$-\log B(\boldsymbol{\beta})+(\beta_0-K)\psi(\beta_0)-\sum_{k=1}^{K}(\beta_k-1)\psi(\beta_k)$	
Graph Posterior Networks (Stadler et al., 2021)	$\psi(\beta_y)-\psi(\beta_0)$	$-\log B(\boldsymbol{\beta})+(\beta_0-K)\psi(\beta_0)-\sum_{k=1}^{K}(\beta_k-1)\psi(\beta_k)$	
Generative Evidential Neural Network (Sensoy et al., 2020)	$-\sum_{k=1}^{K}\left(\mathbb{E}_{p_{\text{in}}(\mathbf{x})}\big[\log(\sigma(f_{\boldsymbol{\theta}}(\mathbf{x})))\big]+\mathbb{E}_{p_{\text{out}}(\mathbf{x})}\big[\log(1-\sigma(f_{\boldsymbol{\theta}}(\mathbf{x})))\big]\right)$	$-\log\frac{\Gamma(K)}{B(\boldsymbol{\beta}_{-y})}+\sum_{k\neq y}(\beta_k-1)\big(\psi(\beta_k)-\psi(\beta_0)\big)$	The main loss is a discriminative loss using ID and OOD samples, generated by a VAE. The regularizer is taken over all classes *excluding* the true class y (also indicated by $\boldsymbol{\beta}_{-y}$).